Estimating Trade-offs for Environmental Flows at the Basin Scale

By

NICHOLAS ROBERT SANTOS

THESIS

Submitted in partial satisfaction of the requirements for the degree of

MASTER OF ARTS

in

Geography

in the

OFFICE OF GRADUATE STUDIES

of the

UNIVERSITY OF CALIFORNIA

DAVIS

Approved:

Jay Lund, Chair

Robert Hijmans

Jon Herman

Committee in Charge

2020

Contents

1 Introduction **1**

2 Background and Model Description **2**
2.1 Environmental Flows . . . 2
2.1.1 Functional Flows . . . 4
2.1.2 California Environmental Flows Framework . . . 4
2.2 Metaheuristics in Environmental Flows . . . 6
2.3 Assessing Trade-offs . . . 7
2.4 Optimizing Environmental Flows . . . 9
2.4.1 Flow Components in Optimization . . . 9
2.4.2 Objectives and Decisions . . . 11
2.5 Summary . . . 12

3 Quantifying Flow Benefits **13**
3.1 Introduction . . . 13
3.2 Background . . . 13
3.3 Methods . . . 14
3.3.1 Single Segment and Day . . . 15
3.3.2 Single Segment, Multiple Species, Single Day . . . 27
3.3.3 Extending to multiple days and reaches . . . 29
3.4 Discussion . . . 30
3.5 Summary . . . 30

4 Estimating Trade-off Curves **31**
4.1 Introduction . . . 31
4.2 Methods . . . 32
4.2.1 Site . . . 32
4.2.2 Interpolating Total Daily Flow . . . 33
4.2.3 Mass Balance in the Stream Network . . . 34
4.2.4 Software and Model Runs . . . 34
4.3 Results . . . 36
4.3.1 Michigan Bar Segment . . . 36
4.4 Discussion . . . 39
4.4.1 Model Performance . . . 39
4.4.2 Model Expansion . . . 41
4.4.3 Potential Adjustments . . . 41
4.5 Summary . . . 42

5 Conclusions **43**
5.1 Future Work 43

Appendices **45**

A Acknowledgements **46**

B Code **47**

C Additional Figures and Tables **48**
C.0.1 Model Verification 48
C.0.2 Michigan Bar 2010 Results 52
C.0.3 Michigan Bar 2011 Results 56
C.0.4 Flow Metrics 62
C.0.5 Michigan Bar Flow Metric Values 63
C.0.6 Species Presence from PISCES 64
C.0.7 Primary Stream Orders 65

References **67**

List of Figures

2.1 Functional flow component illustration 4
2.2 Example trade-off curves for environmental and economic benefit 8
2.3 Optimizing flows using flow components 10

3.1 Simple flow component construction 15
3.2 Fuzzy flow component construction 17
3.3 Single day dry season base benefit 20
3.4 Entire dry season base benefit 21
3.5 Winter peak flow benefit with hydrograph 22
3.6 Peak benefit modifications to base benefit 23
3.7 Recession benefit calculation decision chart 26
3.8 Species Range Downscaling 28

4.1 Map of Modeled Segments of the Upper Cosumnes Watershed 32
4.2 Stream Network Flow Routing 34
4.3 Model E Results for Water Year 2011 37
4.4 Model E Results for Water Year 2010 38
4.5 2010 and 2011 Comparison of Proportional and Optimized Benefit 40

C.1 Cosumnes Model Approach Validation Plot 48
C.2 Michigan Bar Validation Plot 49
C.3 2010 Comparison of Proportional and Optimized Benefit 50
C.4 2011 Comparison of Proportional and Optimized Benefit 51
C.5 Model E Results for Water Year 2010 with Random Seed 20200224 . . . 52
C.6 Model E Results for Water Year 2010 with Random Seed 912264360 . . . 53
C.7 Model E Results for Water Year 2010 with Random Seed 34578239 . . . 54
C.8 Model E Results for Water Year 2010 with Random Seed 793539823 . . . 55
C.9 Model E Results for Water Year 2011 with Random Seed 20200224 . . . 56
C.10 Model E Results for Water Year 2011 with Random Seed 912264360 . . . 57
C.11 Model E Results for Water Year 2011 with Random Seed 34578239 . . . 58
C.12 Model E Results for Water Year 2011 with Random Seed 793539823 . . . 59
C.13 Full Michigan Bar 2011 Environmental Objective Convergence 60
C.14 Full Michigan Bar 2011 Economic Objective Convergence 61

List of Tables

2.1 Environmental Flow Assessment Methods 3

3.1 Flow metrics used in piecewise benefit equation 18
3.2 Probabilities of species presence by stream order 29

C.1 Modeled flow metrics used to construct fuzzy flow component benefit . . 62
C.2 Michigan Bar Flow Metric Values 63
C.3 Species present on modeled stream segments 64
C.4 Primary Stream Orders for Wide Ranging Fish Taxa 65

Abstract

The California Environmental Flows Framework (CEFF) developed new guidance and tools that use functional flows to establish environmental flow requirements. To support that process we developed a new, simplified method to evaluate the ecological benefit of a potential functional flow regime. We used the method in an evolutionary algorithm-based optimization model to produce optimized economic/environmental trade-off curves. Trade-off curves inform the best likely consequences of deviating from flows recommended in the CEFF process, supporting a second, more social balancing, phase of developing environmental flow requirements. We applied the model to water years 2010 and 2011 on the Cosumnes River watershed in California, but the same methods could be used elsewhere provided data are available. Larger models failed to converge in a reasonable time period, but a single segment model produced an optimized functional flow timeseries and trade-off curves.

Chapter 1

Introduction

Human water use creates pressure on aquatic ecosystems, which are in decline in California and globally (Moyle et al., 2013; Howard et al., 2015; Dudgeon et al., 2006). Withdrawals of water stress river ecosystems in a variety of ways and river flow management must balance withdrawals with maintaining enough water in streams to sustain ecological functions. The reservations of water to support ecological functions are generally referred to as environmental flows (Arthington, 2012). Since at least the 1940s, numerous methods have been developed to determine the river flows required to support ecosystem function. Many methods employed in these environmental flow assessments (EFAs) focus only on maintaining a minimum flow in river systems instead of understanding and supporting all major ecosystem functions. In recent decades, there is increasing interest to recreate features and variability of natural flow regimes to provide more effective support for native ecosystems. In California, a new approach to environmental flows assessments uses the concept of functional flows (Yarnell et al., 2015; Yarnell et al., 2020; CEFF Contract Team, 2020).

An environmental flow assessment may be used to establish a set of flow quantity and quality requirements for a river. In some cases, the assessment may require specific reservoir release volumes, while in others, it may specify that the reservoir must release enough water to ensure a downstream objective is met at the correct time, such as connecting a floodplain for fish rearing (Muth et al., 2000; Chart et al., 2007). In any case, the requirements attempt to balance the needs of ecosystems and humans.

Evolutionary algorithms, used in system optimization, could support development of these environmental flow requirements and inform the trade-offs involved in environmental flow requirements. A tool built to help understand trade-offs would have significant applicability in California, where the California Environmental Flows Framework provides a science-based process for establishing the ecological requirements, but where environmental flow requirements will be decided through a social process.

This thesis proposes methods for evaluating the ecological benefit of flows based on the functional flows approach and a model and reusable tool that optimizes environmental flows and water extractions for every stream segment in an entire basin. The goal is to support the social process of setting environmental flow requirements by producing trade-off curves that can inform the consequences of deviating from recommended flows. It includes a sample application for the Cosumnes River watershed in California, but the same process and software could be used elsewhere in the state provided data are available.

Chapter 2

Background and Model Description

We begin by exploring the history of environmental flow assessment and its current application in California, including the use of optimization algorithms to inform environmental flow options and management.

2.1 Environmental Flows

The flow regime of rivers is most commonly characterized with hydrographs using measures of magnitude, timing, duration, frequency, and rate of change (Poff et al., 1997). Early environmental flows emphasized simple minimum flows, but eventually encompassed broader ecosystem objectives and variability (Tennant, 1976; Poff et al., 1997). Tharme (2003) broadly characterizes environmental flow management techniques into six categories: hydrological, hydraulic rating, habitat simulation, holistic (ecosystem), hybrid, and "other" methods (Table Table 2.1). No single method dominates environmental flow development. Tharme (2003) found 207 methods globally for establishing environmental flows. At that time, minimum flows were the most common and Arthington (2012) notes that 70 percent of published flow setting methods use non-holistic techniques despite their well-known weaknesses in not supporting broad ecosystem function.

As Poff et al. (1997) observed, natural variability drives ecosystems, and not simple averages. By 2007, it was well established that interannual variation is critical for systems (Mathews and Richter, 2007). Holistic methods attempt to preserve important characteristics of the original flow regime's variation, even while allowing extractions of water. Since their development, holistic methods have received the most attention, in part because the analysis often encompasses tools used in hydrologic, hydraulic rating, and habitat simulation approaches (Tharme, 2003).

Some recent methods in the literature focus on hydrologic alteration as a basis for establishing environmental flows. Mathews and Richter (2007) write that often, determining the degree of hydrologic alteration is useful because it requires understanding pre-alteration conditions that the ecosystem is adapted to and how far the system has deviated from this baseline. They suggest that this information "can focus flow protection and restoration activities, provide direction for ecological research and monitoring, and identify priority management actions" (Mathews and Richter, 2007, p. 1401).

A prominent holistic process is described in the Ecological Limits of Hydrologic Alteration (ELOHA) framework (Poff et al., 2010; Kendy et al., 2012). The framework involves four main components, each having detailed steps:

Table 2.1 Description of the six primary types of methods used to establish environmental flows. Adapted from Tharme (2003) and Arthington (2012).

Technique	How it sets flows
Hydrological	Relies on hydrologic data and typically sets a minimum flow. Occasionally uses quantity or quality of upstream habitat to set flow requirements.
Hydraulic Rating	Uses cross-sectional measurements of hydrologic variables, such as wetted perimeter or depth. These measurements are plotted against discharge to find flows needed to maintain habitat at sufficient quality and quantity.
Habitat Simulation	Analyzes the amount and quality of instream physical habitat available at different flow levels.
Holistic	Modifies and preserves elements and features of the original flow regime, using resulting hydrograph to set flows.
Combined or Hybrid	Incorporates aspects, concepts, and tools from more than one of the other methods.
Other	Designed for other purposes but adapted for use in EFAs.

1. Obtain the "hydrologic foundation", or the current flows and conditions
2. Classify river types to apply lessons for studied rivers to new places
3. Establish flow-ecology relationships, which help understand how flow alteration affects ecological condition.
4. Set goals for a desired future condition

Following the official steps, ELOHA feeds into a social process of evaluating societal values, management needs, and acceptable levels of alteration to ecology in setting environmental flow allocations. The result includes information both on what flows the ecosystem needs and how much society is willing to provide, with a process that recognizes the inherent tension between the two objectives.

The ELOHA framework is location agnostic and each implementer appears to construct the components of the framework differently (Kendy et al., 2012). For example, Kendy et al. (2012) describe nine case studies and show that in each case, the implementation uses different data and processes to build each component of ELOHA. In addition, Sanderson et al. (2012) built a tool as part of a pilot for parts of Colorado called the Watershed Flow Evaluation tool, which could have supported more standard application of ELOHA. While they describe the tool as generalizable to other locations, no code or tool is publicly available.

2.1.1 Functional Flows

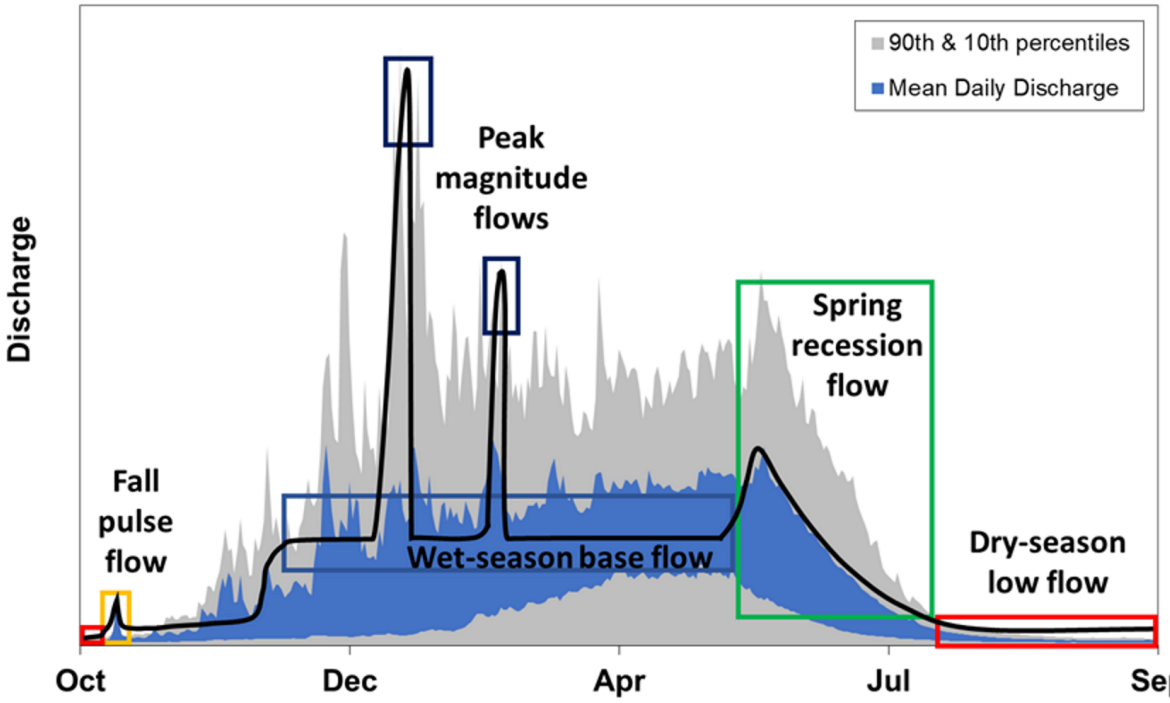

Figure 2.1 Functional flow components illustrated over a reference hydrograph. The dark line represents example manufactured functional flow regime during a moderate water year. Adapted from Yarnell et al., 2020.

Current environmental flow discussions center on more complete characterizations of flows, such as "functional flows". Functional flows mimic characteristics of unimpaired flow most vital to the ecosystem while still allowing for human withdrawals and alteration (Yarnell et al., 2015; Yarnell et al., 2018). Functional flows support major functional elements, processes, and signals of a river system to benefit the whole ecosystem. Rather than recreating historical flows, instead "flow components" such as "winter peak flow", "spring recession" and "summer base flow" support critical ecosystem and geomorphic processes.

Components distill variation of a hydrograph into a set of defined boxes that represent specific assessed flow needs of the ecosystem, as seen in Figure 2.1. A typical functional flow attempts to provide flows within each functional flow component box during a water year to support the ecosystem function each box represents (see black line in Figure 2.1). As a result, flow components provide targets for water managers during environmental flow development and operations, identifying important hydrograph behavior along with the flexibility to extract or modify higher flows.

2.1.2 California Environmental Flows Framework

Recently, the State of California embarked on an effort to establish environmental flow requirements statewide. The initiative, called the California Environmental Flows Framework (CEFF), uses the approach outlined in Yarnell et al. (2020), which complements the ELOHA process but is adapted to address the difficulties in collecting the data ELOHA

requires at the statewide scale. The use of functional flows avoids the need to develop explicit flow ecology relationships for each stream reach because the authors assume matching historical flows through functional flows broadly supports instream ecology.

CEFF draws on the concept of functional flows proposed by Yarnell et al. (2015) (see Figure 2.1). The effort conceptualizes flow components in terms of their "boxes", defined by the timing, duration, and magnitude of a described flow, such as summer baseflow. The boxes are defined by a set of values called metrics defined by historical quantile values for hydrograph characteristics like timing, magnitude, and duration (eg: 10^{th} percentile flow magnitude). Peak flow components also require frequency metrics, and spring recession components require rate of change metrics.

CEFF includes five flow components of three core types, each with their own requirements and behaviors (Yarnell et al., 2019).

1. Baseflow components assess whether the segment has enough flow compared to historical data. They consider flows based solely on whether the flow is within historical ranges of magnitude, timing, and duration. The dry season and wet season each have baseflow components.

2. Peak components require magnitude and timing as with baseflow components, but require more variability and higher magnitudes. A functional flow that stays locked in peak flow would be less beneficial, or possibly even detrimental, than a functional flow that includes peak flows but returns to baseflow after individual high flow events. Fall and winter each have separate peak components, with a single flushing flow for fall while the winter peak flow can occur many times based on modeled frequency data.

3. Recession components focus on rate of change as flows decrease, typically from winter rain and snow into summer baseflow. Flows must still be in historical timing and magnitude ranges and must also maintain a daily rate of decrease matching ecosystem needs. Currently a single recession component covers spring transition from winter to summer flow.

During an environmental flow assessment, agency staff using CEFF will assess alteration from baseline conditions by comparing flow metrics for each of these components to modeled historical values. The authors of the guidance document state that:

> *"The Framework provides guidance on developing ecological flow regimes, given regional or site-specific stream conditions, management goals, and desired ecological outcomes" (CEFF Contract Team, 2020).*

Those using the framework then use the ecological flow regime to develop environmental flow prescriptions. CEFF is on track to become the State Water Resources Control Board's standard approach for development of environmental flows, making a consistent process statewide that supports the state's broad water resilience objectives (California Natural Resources Agency et al., 2020).

Like ELOHA, CEFF expects that the data and modeling collected when developing environmental flows will be used in a social process with stakeholders that determine how the science is used and applied. While the CEFF process itself provides the ecological flow regime, the development of environmental flow prescriptions will often require an understanding of the trade-offs or consequences of deviating from the ecological flow regime.

2.2 Metaheuristics in Environmental Flows

Optimization tools are a promising approach to developing information on trade-offs. Optimization has a deep history in environmental flows, particularly with the use of linear programming and metaheuristics. Metaheuristics is a subfield of stochastic optimization frequently applied to what Luke (2013) describes as "I know it when I see it problems." In such problems, the quality of the solution can be readily evaluated, but inputs required to generate a good solution are imperfectly known, either due to complex interactions, or incomplete knowledge about inputs. In an environmental flows context, this would mean that it is possible to recognize a near-optimal flow, but less is known about which pieces of the system of study should be adjusted to obtain that flow. More broadly, in water resources, metaheuristics has been used for model calibration, planning, design, and operations (Maier et al., 2014). They have been applied to problems of water distribution, groundwater management, river-basin planning and management (Maier et al., 2014).

Evolutionary Algorithms (EAs) are a specific type of metaheuristic drawing inspiration from evolutionary biology. An EA uses random variations combined with a fitness function that evaluates potential solutions to converge on a near-optimal result. These algorithms are well-suited to situations where potential outcomes may conflict with each other, making them useful in environmental flows where allocation of water in one location may reduce water available elsewhere (Horne et al., 2016).

Maier et al. (2014) detail the history of metaheuristics in water resources, noting their increased use since 1991 when they were first applied to water optimization. The authors note that EAs have a few advantages over other optimization tools:

1. Their underlying concepts are easy to understand.
2. They are easy to add to existing simulation models, reducing the need for problem simplification
3. They support parallel processing, allowing them to take full advantage of available computing power.
4. They are adaptable to many problem spaces and contexts that support an "explore and exploit" strategy that searches the whole problem space and narrows in on near-optimal solutions.

Literature on environmental flow optimization appears dominated by reservoir operations research, and Horne et al. (2016) explicitly note that "many of the operational models were developed for optimizing environmental releases from hydropower dams." The authors found that most studies (27 of 42) used a metaheuristic, usually evolutionary algorithms. Linear and mixed integer linear programming models were the next most common, with 8 studies, and non-linear and dynamic programming were used in 7 studies. Of these, six studies focused on basin-level optimization, but mostly through reservoir operations. One study focused specifically on flows in California for fish. It maintained a narrow reach scale analysis, but used simulated annealing to estimate optimal flow timing across a water year for fall Chinook salmon in California's Central Valley (Jager and Rose, 2003).

In contrast to other optimization methods, such as linear programming, EAs do not guarantee global or local optimal solutions. However, they can guarantee near-optimal

solutions, given sufficient run time, which will vary by model. Still, their use for environmental flows may help with the more complex relationships among variables, or the types of decisions being made. Relative to linear programming, decision variables for environmental flow problems are often nonlinear. For example, providing additional flow does not produce a known, constant net benefit to species. The benefit can vary based upon other conditions and the current level of flow, and in some cases additional flow can cause benefits to decrease.

2.3 Assessing Trade-offs

To support the social portion of environmental flow development with optimization, consider the general case of trade-offs in resource management. Resource constraints and uncertain outcomes are fundamental challenges for ecosystem managers. A manager may wish to take many actions based on scientific processes, but will need to make decisions based on 1) the values of the resource to each stakeholder, 2) available funds, staff, and other resources, 3) legal requirements, and 4) on the likely outcomes of using resources on any action. Potential strategies to address allocation of resources include expert planning processes (such as Joseph et al., 2009) and computer modeling.

Decision support tools are designed to aid this kind of situation by providing information on many possible outcomes for a range of available choices. Decision support can be as simple as a table of choices and expected results and as complex as interactive graphical applications that a manager can tune to a specification while visualizing results in many dimensions.

Optimization algorithms are a common tool for decision support. They typically find optimal choices or reduce the problem space by removing infeasible or objectively bad results, providing a set of choices to examine based on other criteria. Specifically, a multi-objective optimization model can reveal trade-offs among available choices, allowing for a better understanding of the costs and benefits of particular choices.

Imagine a simple case where we can allocate water for environmental uses or economic activities such as farming, industry, or municipal uses. In a few cases, water allocated to one can support the other, such as in many ecotourism activities, but in most cases, water allocated to one cannot benefit the other, resulting in a trade-off. A trade-off can be as basic as a linear relationship, such as one unit of water allocated to the environment produces one unit of environmental benefit and removes one unit of benefit from economic activities. In many cases, the relationship will be more complicated than a one to one trade-off, and can have interesting features that guide decisions, such as curves, kinks, and benches.

Null et al. (in review) describes an approach to determining whether specializing streams or stream reaches by purpose could yield improved outcomes. Using multi-objective optimization, a trade-off curve, or Pareto front, of environmental and economic benefits can be derived for each unit of study, such as a stream segment. The shape of this curve would guide whether specialization of the segment or compromise between interests is the optimal outcome for a set of streams or stream reaches (see Figure 2.2). If the curve is convex, as in the solid curve on Figure 2.2, then a single unit increase in benefit for either economic or environmental purposes comes at great cost to the benefit of the other objective. As a result, managers have incentive to specialize that stream segment and others like it, dedicating some for economic purposes and some for environmental

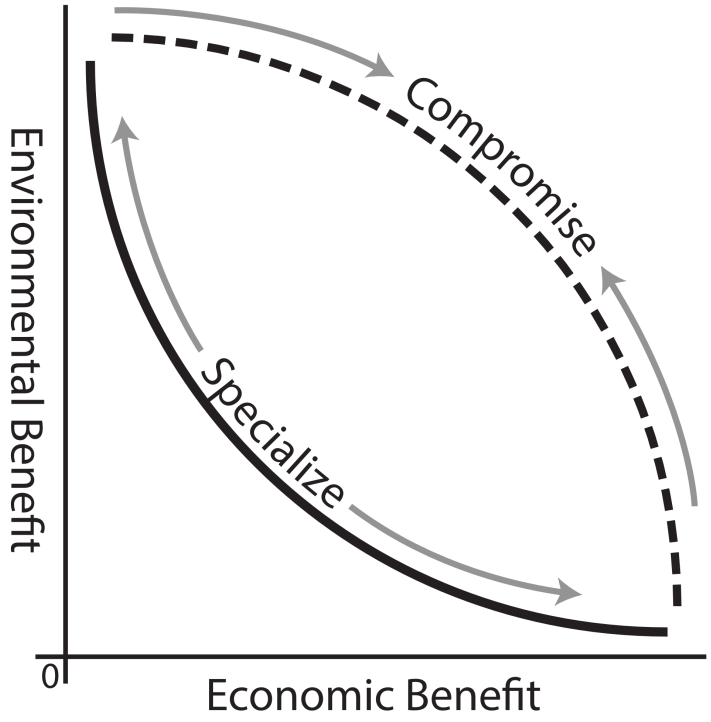

Figure 2.2 Example trade-off curves in watersheds for environmental and economic benefits and their implications for management. Arrows point in the direction of maximum benefit along each curve. Adapted from Null et al. (in review).

purposes. For this specialization, they would achieve a higher total benefit because the benefit to each under compromise is low.

However, if the curve is concave, as in the dashed curve on Figure 2.2, then economic and environmental benefits are maximized through compromise on each stream or stream reach. Each unit of increased benefit to one objective comes at relatively little cost to the other objective. Such a situation creates incentive to maximize benefits by balancing the objectives in the same subwatershed. In some cases, curves will have other features – small benches or variation caused by thresholds. For example, there may be a minimum flow before the environment sees any benefit or before it is economically feasible to extract water. Alternatively, at higher levels of environmental flows, floodplains could connect, causing a disproportionate increase in environmental benefit. These features also inform management, though the core strategy will be directed by the overall shape of the curve as shown in Figure 2.2.

Instead of a tool that finds an optimal allocation of water for each purpose this thesis describes a tool that builds trade-off curves. The goal is to inform management where existing environmental flow processes, such as CEFF, have already informed the best environmental allocation via the ecological flow regime. The trade-off curves would then be used as part of the social process that sets the environmental flow prescription, providing information on the consequences of deviating from the best allocation to support other goals. Other optimization tools in California may provide similar information at a larger regional scale, such as CALVIN (Draper et al. (2003) and Dogan et al. (2018)), but typically are focused on infrastructure operations rather than environmental requirements.

Purkey et al. (2018) note that stakeholder processes increasingly drive water resources decisions in the United States and the growing recognition that deterministic models may be inadequate in the face of uncertainty. These two factors combined suggest that models and approaches that provide many possible outcomes, instead of a single true result, could be strongest. A model that produces many possible results can acknowledge its own uncertainty and give stakeholders options as they weigh factors not incorporated into models. The decision making model presented in Purkey et al. (2018) includes steps for options analysis and results exploration, while the framework they built their model on includes an explicit step to assess trade-offs.

Others have approached similar problems with differences in place, scale, and specific methods. Homa et al. (2005) developed a method to assess the performance of environmental flows relative to water supply reliability. The result includes four options they describe as the start of a Pareto front. Maloney et al. (2015) developed a decision support application that evaluates and compares many scenarios. Its primary difference is that it appears to operate at more localized scales rather than supporting basin-scale decision making. The most similar recent work is by Zamani Sabzi et al. (2019) and compares two objectives of "environmental satisfaction" and "societal satisfaction" in the Red River Basin. They developed multiple Pareto fronts with a linear program that adjusts societal water needs to inform how conservation can improve available decisions (similar to Rheinheimer et al. (2012)). They also model an entire basin's reservoir releases using water rights data to inform societal demand and a minimum instream flow requirement for environmental flows.

2.4 Optimizing Environmental Flows

2.4.1 Flow Components in Optimization

An optimization model that supports CEFF would attempt to optimize flows so that they fall within the boxes for each flow component as much as possible, while allowing for water extraction. The results of a hypothetical optimization for a single stream segment over a water year are shown in Figure 2.3. The figure shows the water year 2018 hydrograph for Goodyear's Bar in gray, environmental flow allocation generated by the model in black, flow components in the boxes, and "base benefit", the hypothetical calculated value of the flow to the ecosystem in the top graph.

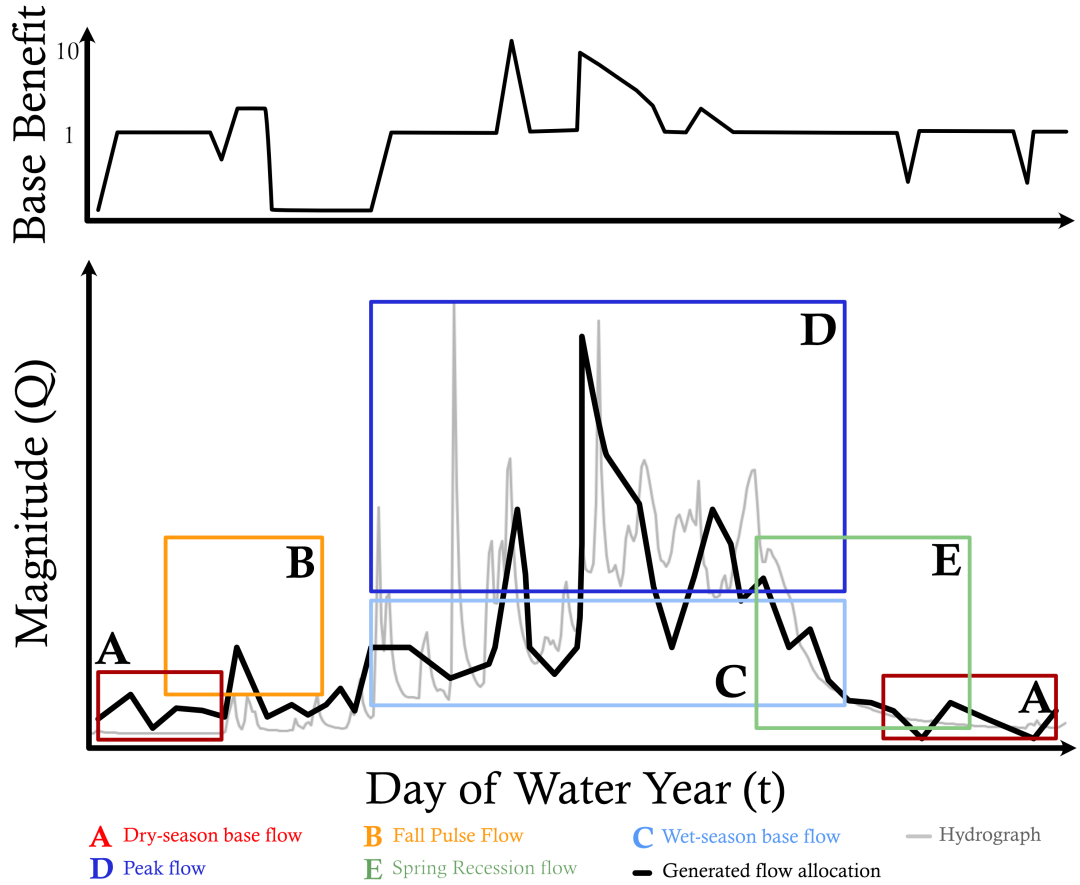

Figure 2.3 Hypothetical results of an optimization model run calculating the daily benefit to the ecosystem of the flows shown in the black line, based on the flow components shown in the boxes. The Base Benefit quantity in the top panel assesses how well flows align with historical flows in timing, duration, and magnitude and is used as a multiplier along with species presence data to general a total benefit of annual flows.

Figure 2.3 contains a few differences in its illustration of flow components compared to the example in Figure 2.1. First, the component boxes tend to be much larger, especially for the peak events. Where the first figure shows discrete peak events, the hypothetical results show the entire range of time and magnitude where peak events could occur, based on probabilistic models from Grantham et al., in prep. Second, the environmental flow allocation (lower black line) in the first figure is a final flow regime while in Figure 2.3 it is a flow regime that evolved semi-randomly for evaluation in a model. It represents one of very many potential flows generated by an evolutionary algorithm in an optimization context. The top line is the benefit calculated by the model for this particular hydrograph. It provides a daily benefit value of 1 for flows within baseflow boxes or for flows that match spring recession requirements, with small spikes in value above 1 for peak flows. The peak value tails off to incentivize return to baseflow. Specifics of these calculations are described in chapter 3. The power here is that while, given the right data, a human can quickly draw one functional flow regime, the computer can evaluate millions of functional flow regimes across thousands of stream segments while accounting for the effects and constraints of one functional flow on another, as well as on economic withdrawals of water.

In evaluating many potential flow regimes, an evolutionary algorithm can find options that perform best across a region or basin.

2.4.2 Objectives and Decisions

To build trade-off curves from the single segment environmental benefit in Figure 2.3 we formulate a basin-wide optimization problem with objectives maximizing environmental benefit (Equation 2.1) and economic benefit (Equation 2.2). Each objective has one decision variable for the total flow volume or percent allocated to its exclusive use from the available water. The model uses a basin-wide hydrologic network that ignores existing infrastructure. Instead of optimizing reservoir releases or extractions, the model assumes operators make a decision to withdraw water or not withdraw water on every stream segment. It uses withdrawn water for economic purposes and instream water for environmental flows. The instream flow also flows downstream where the same choice is repeated again. In analyzing basins in this way, we explore possibilities for the future of the system rather than developing optimal operating rules or instream flow requirements directly. Evolutionary algorithms are well-suited to this task because they can explore and exploit the realm of possible options. They conduct a wide sample of the whole set of physically possible options and then refine the better performing ones. With such information, we can build trade-off curves (Pareto fronts) to better understand the consequences of both major and minor changes in decision variables.

$$\textit{Environmental Benefit} = \sum_{d=1}^{365} \sum_{s=1}^{n} B(d, s, P_{ds}) \tag{2.1}$$

where

$\textit{Environmental Benefit}$ = Basin-wide environmental benefit
d = Day of water year
s = Stream segment
P_{ds} = Proportion of daily flow reserved instream for stream segment

Initial basin environmental benefit uses independent decision variables for proportion of flow reserved for instream use. Within the benefit functions the independent variables are connected via a mass balance calculation. Total basin benefit is calculated by the sum of benefits for individual stream segments for each day of the water year. Adams (2018) describes several alternative ways of aggregating environmental benefits over time and space, and their importance. The approach used here does not account for habitat fragmentation and may be more appropriate for ecosystems dominated by species residing in single river reaches, not migrating across reaches. The environmental flow benefit calculation in Equation 2.1 is a function of the day of the water year (d), stream segment (s), and water allocated to environmental flows for that segment and day ($Q_{d,s}$), calculated for every day and stream segment, then summed to calculate the benefit across the entire basin of study. The function B is detailed in chapter 3. Water dedicated to instream flows is available for downstream use for instream flows or extraction.

$$Economic\ Benefit = \sum_{i}^{Q} -\frac{P}{D} * q_i + P \tag{2.2}$$

where

$$\begin{aligned} Economic\ Benefit &= \text{Basin-wide economic benefit} \\ P &= \text{Price of the first unit of water} \\ D &= \text{Total demanded units of water} \\ q_i &= i^{\text{th}} \text{ unit of extracted water} \\ Q &= \text{Total units of water extracted} \end{aligned}$$

Water not dedicated to instream flows is extracted and pooled across the basin for the entire year to calculate a total water diversion. Economic benefit is calculated as the sum of payments for demanded water in the basin, implemented as a linear demand curve using the price for the first unit of water and the desired number of units. Equation 2.2 describes the demand curve based on the price, P, for the first unit of water delivered and total units of water desired from the basin, D. When the total units of water extracted, Q, equals or exceeds D, then P is 0 as well because no more water is desired. The models sums the price of water for all units extracted to calculate total economic benefit of the diversion.

The algorithm will maximize economic and environmental benefit across the whole basin and produce a basin-wide trade-off curve, but an important byproduct of the optimization's structure is localized trade-off curves. We expect basin-wide trade-off information from plotting the Pareto front of the complete optimization, but in the process, we will also have developed trade-off curves for each stream segment in the watershed. This works where basin performance is a summed aggregation of reach performance. Some curves may explore the performance space better than others since the algorithm is not optimizing for each segment on its own, but they are likely to provide useful information on localized trade-offs, regardless.

2.5 Summary

Optimization approaches have a deep history in water resources and environmental flows assessment, including the use of metaheuristics in particular (Maier et al., 2014). A model that evaluates performance of both economic and environmental benefits for an entire basin would be useful during a social process applying the science of environmental flows to policy. The next chapter describes the internal workings of the environmental benefit objective function shown in Equation 2.1 and the following chapter uses the objective functions in an optimization to produce trade-off curves for the Cosumnes River watershed for multiple demand water demand scenarios.

Chapter 3

Quantifying Flow Benefits

3.1 Introduction

In the previous chapter, the environmental benefit objective expressed in Equation 2.1 included a double summation of another function B that accepts parameters for each day of the water year, the stream segment, and the decision variable of flow on that day for the stream segment. This chapter describes how the function B uses those values to assess environmental benefit on a single segment and day, which is then summed to assess total benefit in the objective function. This common approach to assessing basin environmental benefit might not be appropriate for some ecosystems, such as those driven by migratory species whose success in a stream reach for a period of time is driven by their survival and prosperity well beyond that time, which can be driven by a combination of the worst conditions experienced (say high temperatures affecting survival) and their growth during that period, perhaps based on cumulative food availability. Those factors are not explicitly included in this model, though the functional flows approach the model is based on restores processes that may provide broad support for river-dependent species (Yarnell et al., 2020).

3.2 Background

Recent work by Patterson et al. provides methods for identifying characteristics of hydrographs given historical flow data and includes the ability to produce metrics describing those characteristics (Patterson et al., In Review; Lane et al., 2019). The authors built software to assess annual flow data to estimate where features occur and generate flow metrics, such as a the 25^{th} percentile spring magnitude or the 50^{th} percentile dry season start timing. Grantham et al. (in prep) interpolated the flow metric calculations to all stream segments in the state. While the functional flows approach assumes that matching historical flow components using flow metrics benefits the ecosystem, it does not define a single way to construct flow component boxes from historical data, or define how to calculate benefits to the ecosystem from flows in the boxes.

To support setting environmental flow requirements, we need to establish how valuable or beneficial a particular flow is at a time and place. A capability to quantify the benefit of a flow underlies flow optimization. This chapter outlines an initial method to establish flow benefits, using modeled historical flow information as a guide for flows' benefits to

ecosystems. The chapter starts with a single day's flow on a single river segment and moves to discuss evaluating benefits over a river basin and over an entire year.

3.3 Methods

The model establishes benefit in pieces by assessing a hydrograph's alignment with constructed flow components. Conceptually the approach is a type of hydrograph alteration assessment, with hydrographs that are unaltered relative to the historical flow components receiving high scores and highly altered hydrographs scoring lower. The model operates at the scale of stream segments as defined by the National Hydrography Dataset (NHD) (Corporation, 2018) because relevant flow metrics are available at this scale from Grantham et al. (in prep), biological data from PISCES (Santos et al., 2014) can be adjusted to this scale, and stream segments are relevant to environmental flow decisions. California has approximately 130,000 stream segments, which span the distance between any two stream junctions and so vary in length. As a fundamental calculation, the model compares a water year hydrograph after water has been withdrawn for a stream segment against the segment's flow components. The model makes separate assessments for each of the five CEFF components, but examines daily flows and returns values as a daily timeseries for each flow component. After aggregating the flow benefit values for the year, the model then multiples the calculated benefit value by the number of fish species assumed to be present to increase the biological relevance of the flows. The multiplication ensures that segments that support more species receive additional importance in the model.

3.3.1 Single Segment and Day

Building Components and Establishing Benefit

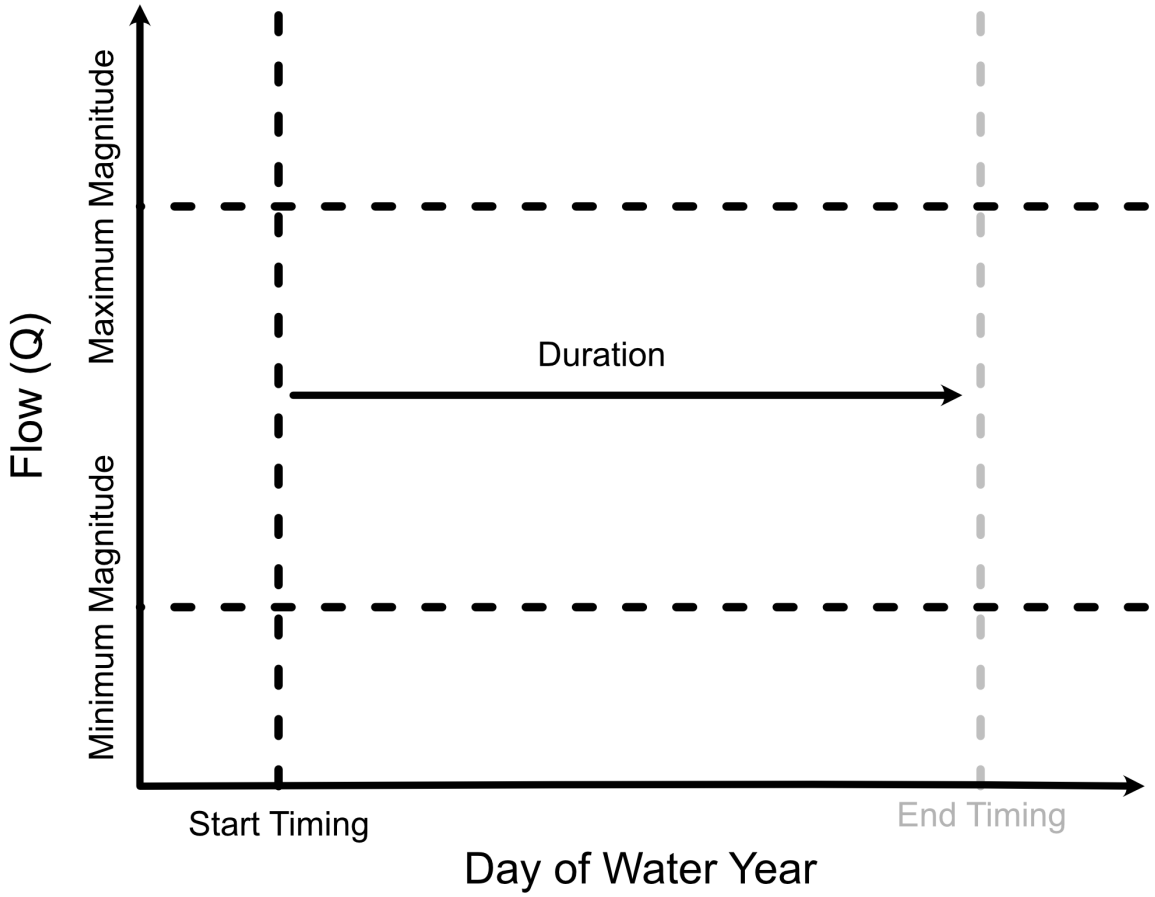

Figure 3.1 Simplified diagram of how a flow component is built from magnitude, timing, and duration data. The minimum and maximum magnitude values establish the lower and upper flow values. The start timing value establishes the first day of the water year for the component, and adding the value for the component's duration to the start timing value results in the end timing for the component, or the last day of the water year it occurs on.

To assess the segment-specific daily benefit of a flow, we first need to build a structure for a segment's flow components in code. Each flow component needs, at a minimum, values for the start day of the water year, end day of the water year, minimum flow magnitude, and maximum flow magnitude. In practice, we use magnitude (CFS), start timing (day of water year), and duration (days) values, constructing the end timing by adding the duration and start timing, as seen in Figure 3.1.

In a simple case where we assume we know the start timing and duration exactly, a wet season baseflow might start on day 50 of the water year and extend for 150 days. In this case, if we add the duration to the start timing, the end day is 200, yielding an X domain (timing) for the flow component box of (50, 200). The X domain gets slightly more complicated for dry season flows. A dry season base flow component might start on day 275 of the water year, and also have a duration of 150 days. When the duration is

added to the start timing, it exceeds 365, and extends into the next water year. In this case, we roll the end day over to the next water year and the component ends on day 60 of the water year (275 + 150 - 365 = 60), yielding an X domain for the component of (275, 60).

The Y domain (flow) of the box has no rollovers. For a baseflow with a minimum flow value of 10 CFS and maximum value of 200 CFS, the Y domain is simply (10, 200). Combining the X and Y domains gives us a simple flow component as in Figure 3.1.

Flow components can represent variable, continuous, and uncertain flow processes. So far, the method described here reduces the component to a fully deterministic box, where flows inside the box in time and magnitude mean the component is happening and flows outside the box mean it is not. Actual flows are more variable and imprecise, varying in time, magnitude, duration, frequency, and rate of change, so we need a mechanism to capture some of that variability.

Fuzzy sets are a concept used to incorporate qualitative reasoning and flexibility into models with wide use in environmental and ecological systems (Salski, 2003). Fuzzy sets allow us to distinguish between flows that match a flow component and those that do not, with a gradual transition between the two states. The gradual transition better reflects the natural state of flows where more extreme values get increasingly less likely, but typically do not have hard thresholds.

Fuzzy sets are not new to environmental flow assessments. In many cases, they are used to support habitat suitability assessments, (e.g. Jorde et al., 2001; Sun et al., 2015; Ahmadi-Nedushan et al., 2008). In another case, Lowe et al. (2017) incorporate uncertainty into environmental flows using fuzzy sets. Young et al. (2000) built a decision support system that allows users to specify fuzzy values for multiple aspects of flow for each species.

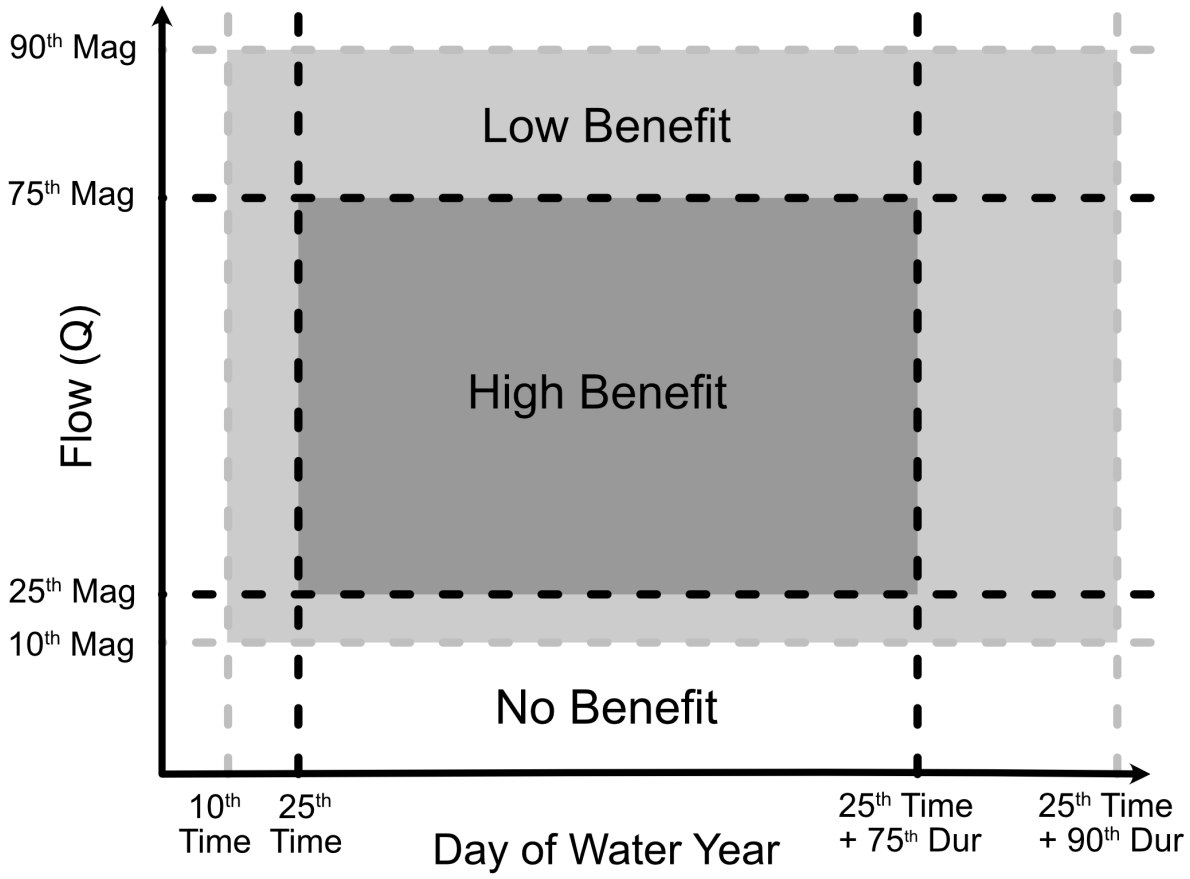

Figure 3.2 Example construction of benefit regions based on flow magnitude and day of water year, based on flow metric values marked on each axis. Shaded regions result from the bounds created by these flow metrics. The model assumes differing benefit to the ecosystem from flows in each region.

To use fuzzy sets in building flow components, we use modeled flow metrics from Grantham et al. (in prep). They calculated and interpolated flow metrics from unimpaired gage sites to every stream segment with a random forests model that used each segment's hydrogeomorphic classification (from Lane et al., 2017) and the California Unimpaired Flows Database (Zimmerman et al., 2018). The model calculated 10^{th}, 25^{th}, 50^{th}, 75^{th}, and 90^{th} percentile values for each flow metric for every segment. For example, the day of the water year indicated by a segment's 10^{th} percentile start time indicates the component begins earlier in 10 percent of years and later in 90 percent of years. section C.0.4 lists the metrics used to construct each component.

The modeled percentiles expand the view of flow components from boxes with discrete boundaries to boxes with a fuzzy edge. Figure 3.2 shows another way to construct a flow component, similar to Figure 3.1, but where the boundary of the component is a range of values on each side, represented as the area in light gray in the figure. The marked locations on the axis indicate the functional flow metric(s) we obtain the magnitude or day of water year values from.

The most analogous part of Figure 3.2 to the simpler representation in Figure 3.1 would be the central portion defined by the 25^{th} and 75^{th} percentile magnitude values on the Y axis and the 25^{th} percentile timing and the 25^{th} percentile timing plus the

75th percentile duration on the X axis (dark gray, Figure 3.1). Within this area, we assign full benefit to flows because a flow within this box in time and magnitude matches the estimated historical flow quantity and timing. While flows are not more likely to occur in this region than in other regions[1], it does contain less extreme values within the distribution of potential values.

We construct a second box (light gray, Figure 3.1) that fully contains the first box using the 10th and 90th percentile magnitude values for the Y axis and the 10th percentile timing value and the 25th percentile timing value plus the 90th percentile duration value on the X axis. While an expansive view of the component might just use this box as a deterministic boundary (and end up with boxes similar to Figure 2.3 as a result) for defining benefit, this transition zone includes more extreme but still common values for the flow component. We assign less benefit to flows in this region, decreasing with distance from the central dark gray area.

The general approach here of using the modeled flow metric percentiles to establish fuzzy flow components provides the foundation we use to build each type of component. The following sections show the distinct construction, behavior, and examples of three types of flow components.

Baseflow Components

Table 3.1 The flow metrics that provide the values in the generic piecewise benefit equation. For specific metric names from Grantham et al., in prep, see Table C.1.

V	v_1	v_2	v_3	v_4
Flow Magnitude (Q)	10th percentile magnitude	25th percentile magnitude	75th percentile magnitude	90th percentile magnitude
Day of Water Year	10th percentile timing	25th percentile timing	25th percentile timing + 75th percentile duration	25th percentile timing + 90th percentile duration

With a conceptual understanding of how the model calculates benefit based on flow components, we look at the specific calculations. Given a flow magnitude and a day of the water year, it calculates two benefit values - one based on the day of the water year, ignoring flow quantity, and the other based on the flow quantity, ignoring day of water year. Each of these is calculated with a generic piecewise function in Equation 3.1 that varies benefit based on how well the magnitude or day value aligns with historically modeled flow data. Equation 3.1 handles both day of water year D and flow magnitude Q calculations, using the variable V to stand in for both. It uses four breakpoints, v_1 through v_4, to split the piecewise behavior while evaluating the benefit to the ecosystem of parameter *V*. For magnitude benefit, we take the values of v_1 through v_4 from modeled flow percentiles. For the day of water year benefit, the v_1 through v_4 values become days of the water year. Table 3.1 contains the flow metrics and percentiles used for each breakpoint. Equation 3.1 has five segments, the first and last of which are identical. It uses flow magnitude on the Goodyear's Bar stream segment (COMID 8058513) as an example, discussing the calculation of benefit for flow values during dry season baseflow,

[1]We expect 50 percent of magnitude values to fall outside of the box. When combined with timing values, we would expect more than half of values outside of the center box.

$$B(V) = \begin{cases} 0, \ for \ V \leq v_1 \\ \frac{1}{(v_2 - v_1)}(V - v_1), \ for \ v_1 < V < v_2 \\ 1, \ for \ v_2 < V < v_3 \\ 1 - \frac{1}{(v_4 - v_3)}(V - v_3), \ for \ v_3 < V < v_4 \\ 0, \ for \ V \geq v_4 \end{cases} \tag{3.1}$$

shown in Figure 3.3. The logic is the same for day of water year benefit, except it has added logic to handle components, like dry season baseflow, what span two water years and thus have lower v_4 values than v_1 values. Using Goodyear's Bar as an example, the v_1 breakpoint value is 44 CFS, coming from the 10th percentile modeled unimpaired flow metric for this segment in Grantham et al. (in prep). Below this 10th percentile value, the model assigns no benefit (B=0) to flows, since dry season flows less than 44 CFS range from rare to not present in the historical record for this stream segment. The same logic applies to values above v_4, in this case 163 CFS coming from the 90th percentile value for this segment. Flows exceeding 163 CFS are either rare or not observed, so the model assigns no benefit to them for this component and segment.

80 percent of historical flows for the dry season baseflow on this segment are between these values, so the model recognizes flows between v_1 and v_4 (44-163 CFS) as aligning with the historical record and providing ecosystem benefit. It does not assign this benefit uniformly though, but instead linearly ramps the benefit up from 0 to 1 between v_1 and v_2, assigns the maximum benefit value of 1 between v_2 (66 CFS) and v_3 (140 CFS), and linearly ramps back down from 1 to 0 between v_3 and v_4. v_2 and v_3 come from the 25th and 75th percentile modeled magnitude values, respectively, meaning that flows that match the middle half of the flows seen in the historical record receive the top benefit value.

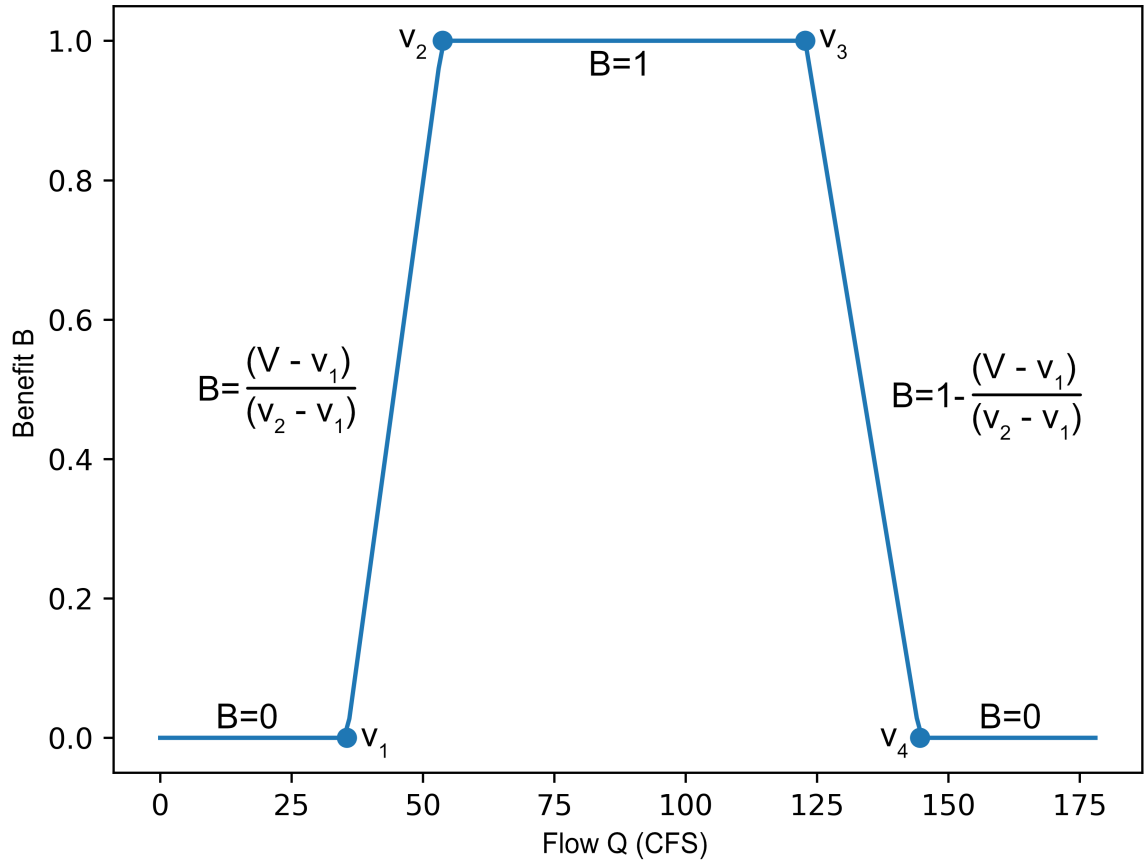

Figure 3.3 Sample dry season baseflow piecewise benefit calculation showing ramp up and down of benefit near the low and high flow values based on flow (Q) values on day 90 of the water year. The breakpoints v_1 through v_4 are labeled, along with the equation used to calculate the benefit value B for each segment.

For timing-based benefits, day of water year values for v_1 through v_4 are based on combinations of flow metric values. v_1 and v_2 are the 10^{th} and 25^{th} percentile day of water year values, respectively, from the corresponding timing metric. v_3 and v_4 are calculated as the value of v_2 plus the 75^{th} and 90^{th} percentiles of the duration metric. When calculated values cross water years, v_3 and v_4 can result in day of water year values *less* than v_1 and v_2, but benefit calculations remain as if they were in order as v_1, v_2, v_3, and v_4. Since the complete baseflow benefit is a function of both flow magnitude Q and day of water year (timing) D, we need some way to combine the timing-based benefit $B(D)$ and the magnitude-based benefit $B(Q)$. We combine them by multiplying them together, otherwise expressed as $B_{base}(Q, D) = B(Q) * B(D)$. If they were summed instead, a flow that was at the wrong time of year but with the right magnitude would still receive benefit when it should not. The result is B_{base}, which is calculated for all component types and is used directly for baseflow components and is modified for peak and recession components. Calculating B_{base} for every day and flow combination in an entire water year provides Figure 3.4, a visualization of the benefit provided by the flow component on any day and for any flow value.

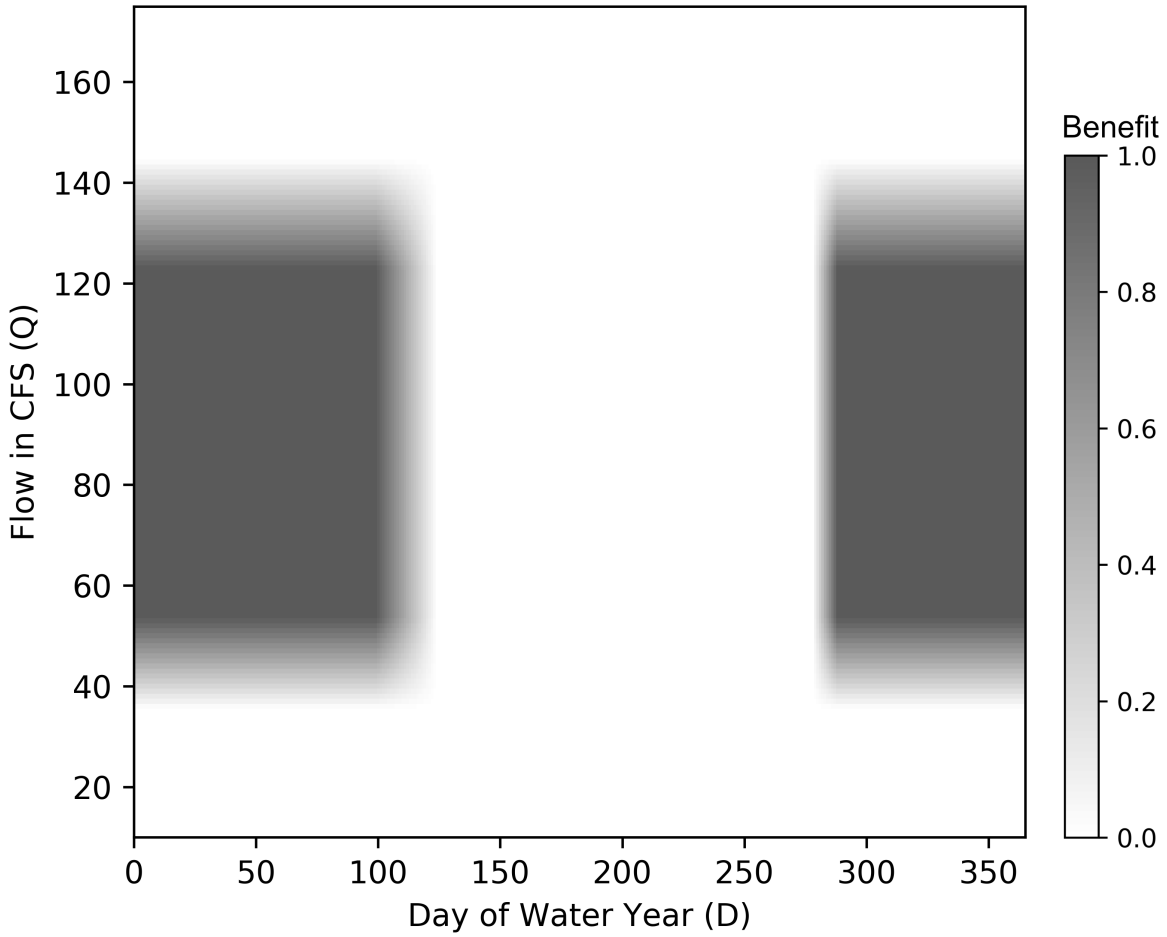

Figure 3.4 Sample benefit box showing ramp up and down of benefit near the low and high flow values for the flow component based on flow (Q) values on day 100 of the water year. Day 100 is between the q3 and q4 values for time-based benefit, so the maximum base benefit is less than 1.

The B_{base} calculation here provides a framework that the other component types can use to alignment of timing and magnitude values of a segment with their modeled historical values. It also provides the raw value used for baseflow components when we include biological data, assess the whole water year, and connect stream segments.

Peak Flow Components

Where baseflows stay in a relatively narrow range for the duration of the component, peak flows are typically more variable and larger in magnitude than the corresponding baseflow for the same time period (see Figure 2.3's Peak and Fall Pulse flows for example). Despite the variability, the flow magnitude typically does not stay high for long, instead returning to baseflow, often in a matter of days.

For example, Figure 3.5 shows the base benefit calculated for the peak flow component of the Goodyear's Bar gage stream segment overlaid with the water year 2018 hydrograph. The peak and baseflow components share timing definitions and only vary in their base benefit, B_{base}, by their magnitudes. The area of high benefit is in the box while the area below would likely be the winter baseflow area.

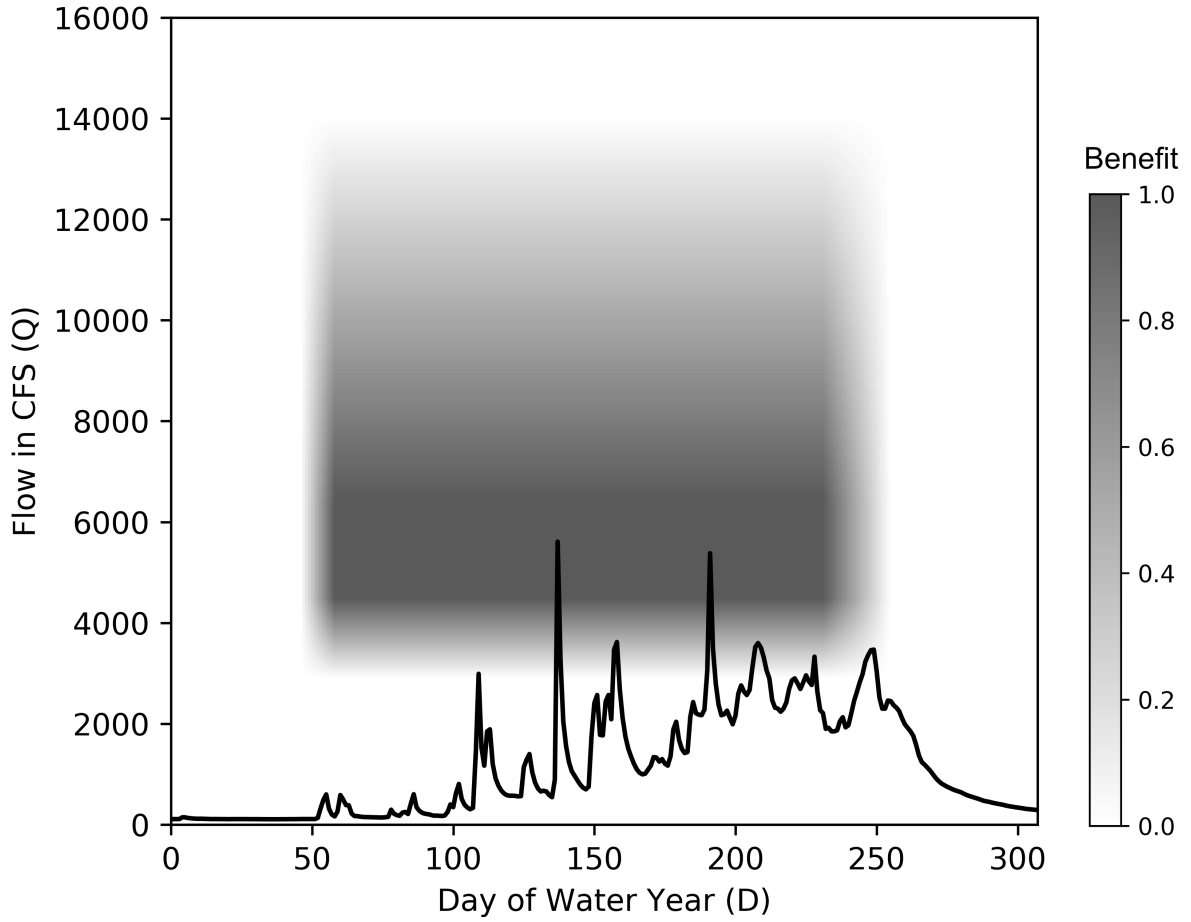

Figure 3.5 B_{base} for the peak flow component of the segment containing the Goodyear's Bar gage overlaid with the water year 2019 hydrograph.

If peak components provided the same benefit as baseflow components we would expect an optimization model testing which flows are best to end up with a relatively even distribution of flows between the peak and base flows for the wet season, absent other incentives in the model. If we want to ensure distinct peak flows, which have geomorphic and ecological benefit, we need to set up a system that temporarily provides more benefit in a peak flow, and also incentivizes a return to baseflows.

Conceptually, to incentivize peak flows, we add additional behavior to peak components that:

1. provides benefit higher than the max baseflow benefit of 1, called B_{max} (initially 10) at least for the first day of peak flows,

2. reduces benefit daily within each individual peak flow event, eventually going below 1 to incentivize a return to baseflow, and reduces B_{max} between flow events to incentivize the correct number of peak events, and

3. multiplies the resulting daily benefit by B_{base} to scale the peak event benefit by how well it matches in timing and magnitude.

The benefit reductions within and between events are controlled by modeled flow metrics from Grantham et al. (in prep) and shown in Equation 3.2. They modeled the duration of individual peak flows separately from the wet season duration (used to

calculate B_{base}) and also modeled the number of peak flow events that typically happen during the wet season (peak frequency). These values contain the same percentiles as the other modeled metrics.

$$B_{peak} = B_{base} * B_{max}^{-R*(L-D)} \tag{3.2}$$

where

B_{max} = Maximum benefit achievable by a single peak flow event
R = Daily benefit reduction factor
L = Length of current peak flow event in days
D = Modeled median peak flow event duration for segment and component

Here we use the median values to reduce benefit, according to Equation 3.2, so that peak events longer than the median event length on that segment will provide less benefit than returning to baseflow would. In Equation 3.2, B_{max} defaults to 10 and R defaults to 0.5.CEFF also provides three peak magnitude metrics for 2-year, 5-year, and 10-year exceedance. We use the 2-year exceedence values here.

Similarly, based on the modeled peak frequency data, we reduce B_{max} linearly between events so after the median number of peak events occur in a single wet season, the model gets less benefit from additional peak events than from continuing baseflow (see right side, Figure 3.6). This behavior reduces the height of the tailoff curve in Figure 3.6 but does not change the length of time the event provides more benefit than baseflow.

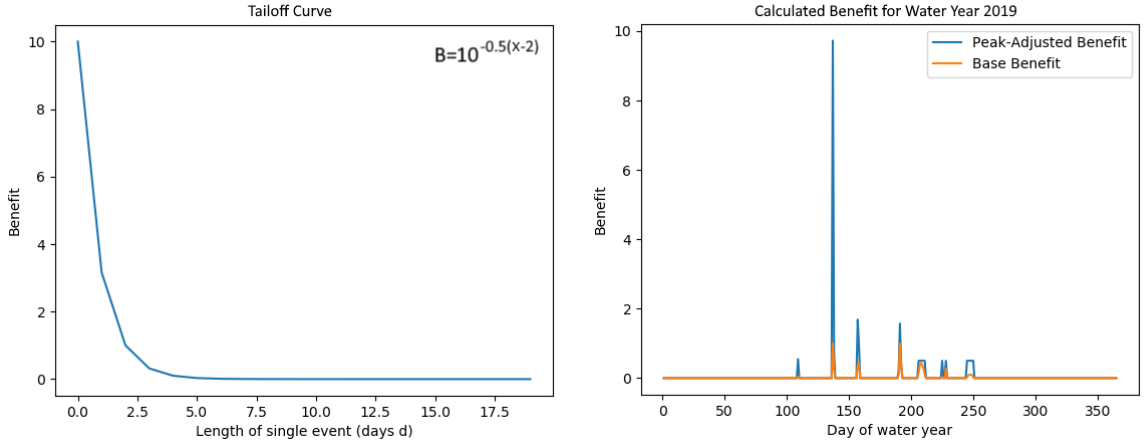

Figure 3.6 Left: The calculated peak flow benefit tailoff curve for Goodyear's Bar, based on modeled flow metric data. Right: Benefit for Goodyear's Bar peak component calculated as if it were only baseflow (orange) or with the peak behavior (blue) based on water year 2019 data. The benefit for peak events initially exceeds 1 to incentivize the model to make peak events, but the value rapidly drops based on flow metric data to make returning to baseflow more beneficial.

One limitation of the current approach is that, conceptually, it may incentivize the model to only ever provide the 25th percentile peak flow where it can get the same benefit as it could with 75th percentile flows. A future modification could use a different gradient from the baseflow calculations that slowly increases into higher percentiles. A gradient would incentivize an optimization model to provide water if it is available, but also allow water for other purposes if needed, increasing the variation in the results.

Recession Components

Baseflow and peak components assume that a flow within the timing and magnitude box means that the component is occurring. Recession flows differ in that, while timing and magnitude remain important, recessions are ultimately about contiguous and low daily rates of flow change. The need to evaluate based on rate of change raises the issue of how long flows should be less than the modeled rate of change values before we consider the segment to be in recession.

Detecting the presence of a recession flow is easy for human eyes examining a hydrograph, but more difficult for a computer (Patterson et al., In Review). A true recession will have a smooth curve from high flow to low flow, but in nature, it can be interrupted early on by late season peak flows, or possibly by diurnal fluctuation in snowmelt. As a result, it can be unclear to a computer algorithm that the portion of time preceding the late peak flow was also part of the recession and that it had been interrupted. Yarnell et al. (2016) describe that recession flows need a minimum of three contiguous weeks without interruptions, such as large peaks and pulses or rapid drops to baseflow, for the stream ecology to benefit. The need for three weeks is driven by the life cycles of organisms, such as amphibians, that use recession flows as signals to reproduce. A peak flow can reset the clock, or wash away egg masses, resulting in a year where the recession did not aid those organisms.

To estimate when a recession is occurring, we look for the longest contiguous period in the water year hydrograph with a daily rate of change less than 30 percent, calculating the daily rate of change according to Equation 3.3.

$$P_{change} = \frac{Q_t - Q_{t-1}}{Q_{t-1}} \tag{3.3}$$

Yarnell et al. (2016) indicate 30 percent is the maximum daily rate of change observed in unregulated systems. Managers risk harm to aquatic communities in higher rates of change and when sustaining 30 percent rates of change over multiple days during the recession. They further specify that rates of change under 10 percent per day are much more likely to benefit the ecosystem. Once a recession period is identified, a benefit is assigned. Similar to peak flows, we multiply the calculation here by B_{base} to scale by recession timing and raw magnitude, but we still need to assess the rate of change. For each day in the recession period, we assess the value of P_{change}, the day's rate of change as calculated in Equation 3.3, as follows:

$\mathbf{P_{change}}$ <0 When the rate of change is less than zero, flows are increasing, so this is not part of a flow recession, whether or not it falls within the recession timing and duration window. So the benefit for the day's recession flow is zero.

P_{change} <0.10 When the rate of change is less than 10 percent the model assigns the full base benefit B_{base} value to the day's flow.

0.10 <P_{change} <90th percentile If the rate of change is not less than 10 percent, but is less than the modeled 90th percentile rate of change for the segment, the model assigns half of the base benefit value. While these values are still reasonable for the segment, reducing the benefit for these rates incentivizes the optimization to allocate flows that produce a rate of recession less than the 10 percent where possible.

0 ≤ P_{change} <0.30 If the rate of change is not in any of the previous ranges, but is still less than 30 percent, the model assigns no benefit for the day.

P_{change} >0.30 A rate of change above 30 percent means that flows are changing rapidly and the benefit of staying at reasonable recession rates on other days can be lost because the recession requires a consistent, slow decline in flows. Under these conditions, we assign no benefit for the entire recession period, eliminating other benefit calculations for other days of the recession. In the absence of this penalty, we might expect an optimization model to have most days with good recession rates while recovering by dropping the flow too sharply to be ecologically safe. By including a harsh penalty for large drops, we can ensure that even if the model drops flows, the rate will be more likely to not take away benefit gained on other days.

The penalty for large rates of change is not applied evenly. Natural variability results in large drops in flow during the peak season with coincident timing to the spring recession component. A penalty that triggered for any large decrease in flow would not encourage development of recession flows in an optimization model. Instead, it assesses if the recession has already begun by calculating the number of continuous days with low rates of changes. With a minimum recession length of 21 days, the model implements the penalty of no benefit across the season if the large drop occurs between 14 and 28 days after daily rates of change first went below 0.30. If a large drop occurs outside of the 14-28 day window, it continues evaluating the rest of the hydrograph for recession benefit.

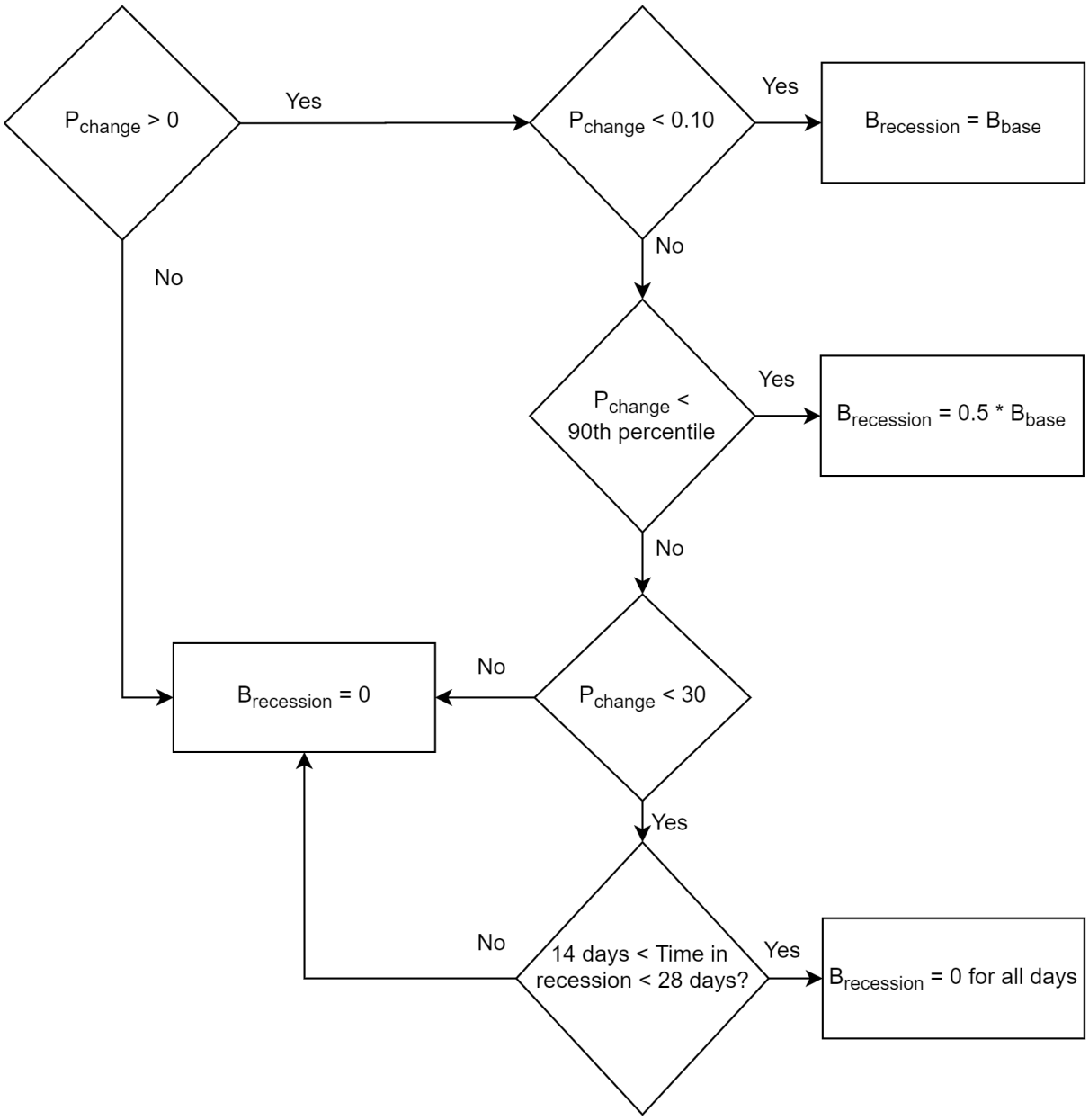

Figure 3.7 Flowchart of daily flow benefit calculation during spring recession. Percentiles refer to modeled rate of change percentiles per stream segment.

Single Segment and Day Summary

In some cases, such as during the wet season, multiple components occur on the same day of the water year. In these cases, to estimate the daily base benefit, we sum the B_{base} of all components that occur that day. This section describes a method for assessing alignment of flows with their historical magnitude, timing, duration, frequency, and rate of change. The assessment is localized to each stream segment and provides a quantity that we call *benefit* and represent as B_{base} for use in modeling applications. In the next section, we scale the benefit quantity according to available biological information to increase its relevance to stream networks.

3.3.2 Single Segment, Multiple Species, Single Day

So far, we have explored a method that estimates the benefit of flows to a segment's ecosystem. As presented, it does not include spatial variations and effects in stream biology in the benefit estimate, limiting its applicability. For example, in an optimization context, imagine two segments that each received the maximum baseflow benefit of 1, but one segment was a high elevation tributary with little life and no fish living in it and the other is a segment of the Sacramento River that supports larger variety of life, including many endangered fish. In such a situation, the biological information informs which segment most needs environmental flows if we cannot provide flows everywhere.

To include biological potential in the benefit calculation, we use the PISCES database (Santos et al., 2014), which provides comprehensive range information for all native fish taxa in California. It may be beneficial to include other organisms in benefit calculations, but currently no complete dataset of presence/absence exists for other aquatic organisms in California. In this case, fish indicate the health of the overall stream ecology.

The PISCES database uses HUC12 subwatersheds to store taxa presence information. These units are coarser than stream segments, necessitating an interpolation of the data before use for stream segment benefit calculations. The simplest form of interpolation would be to say that a species inhabits any stream segment within any subwatershed the species inhabits, producing a more complete picture of the species range, but also a significant overestimate in most cases. A more refined method would be to use species life history traits and flow information for segments to match species to specific segments in each subwatershed, though data to support this kind of calculation would need to be developed.

To reduce overestimation while using available data, we chose a third, semi-probabilistic approach to estimating species presence. The method first estimates which Strahler stream orders a species is likely to inhabit within its range and assigns a probability of presence to each stream order for each fish. It then includes a species as present, at the level of the assigned probability, in each segment within each subwatershed in its range. For example, consider a stream segment with a Strahler stream order of 2 inside the range of a species we estimate is in Strahler stream orders of 3 and above based on PISCES data. For this segment, we do not mark the species as absent, but instead give it a reduced probability of 0.45 for being present, with the calculations detailed below. This method is imperfect, but helps include some uncertainty in interpolation in the final results.

Probabilistic Downscaling

We start by calculating each taxon's *primary stream order*, the stream order value above which we assume the taxon is present and below which we decrease probability they are present. The calculation of primary stream order is based on an assumption that most fish taxa in California will be present in the stream segment in a subwatershed that connects it to the downstream subwatershed, since that segment ensures connectivity of the range. Depending on the taxon, they may or may not be present in other segments, but a conservative estimate that works for most taxa suggests they are at least in this connecting segment[2].

[2]This assumption will not hold for all species. Some are highly endemic, and others like tributaries. But it works as a first pass for downscaling a large dataset and can be refined with more information later.

The segment that connects each subwatershed to a downstream subwatershed will have the largest stream order in the upstream subwatershed. Once we have largest stream order value for each subwatershed, we examine each taxon individually and gather all of the connecting stream order values for subwatersheds within the taxon's range. For each taxon, we select the lowest value as their primary stream order (

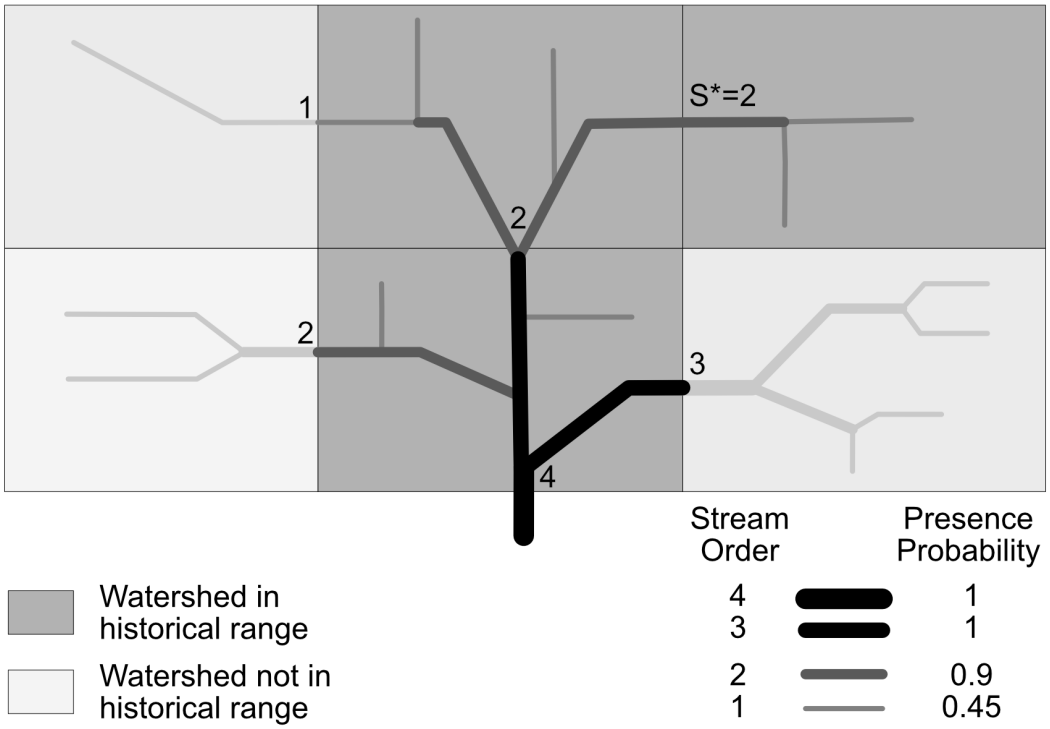

Figure 3.8 Method for determining a hypothetical taxon's primary stream order and assigning probability throughout their range. Size of lines denotes stream order and color denotes estimated taxon presence probability. Numbers indicate the maximum stream order in each watershed. The primary stream order S^* (the smallest maximum stream order in any watershed in their range) for this taxon is 2. Segments outside of their range are ignored.

Once we have a primary stream order value for each taxon, we apply presence probabilistically to all segments within their subwatershed-based range. Any stream segment in their range that exceeds the primary stream order is assigned a presence probability of 1, while segments with the primary stream order are assigned a probability of 0.9 to reflect some uncertainty. Stream segments with smaller stream orders receive smaller presence values according to the function $0.9 * 0.5^{S^*-S}$ where S^* is the primary stream order for the taxon and S is the stream order of the segment being evaluated. Table 3.2 includes presence probabilities for stream segments with Strahler stream orders 1-5 based on this equation.

Table 3.2 Calculated probabilities of fish presence for segments wih Strahler stream orders 1-5 within a species' range if the fish has a primary stream order $S*$ of 1-5.

S^*	S=5	S=4	S=3	S=2	S=1
1	1	1	1	1	0.9
2	1	1	1	0.9	0.45
3	1	1	0.9	0.45	0.225
4	1	0.9	0.45	0.225	0.1125
5	0.9	0.45	0.225	0.1125	0.0563

The calculation marks species as living in larger stream orders within their range while only assigning high probabilities in smaller streams if the taxon's range includes headwater areas with low stream order outlets. The probability values are not empirically derived, but are instead useful in adding some uncertainty to fish presence in each downscaled segment. Future work should refine the methods used to downscale taxa ranges and probabilities assigned. Calculated primary stream orders for every taxon marked as "wide ranging" are included in Table C.4.

Establishing Species Benefit from Segment Benefit

Once the probability that each species is present in a segment is established, the base benefit B_{base} is updated with biological information. The steps to obtain the total benefit B_{total} are:

1. Sum the benefit from each flow component for the day B_{base} to obtain a daily available benefit.
2. Sum all taxa presence probabilities p_{taxa} for the segment to obtain the total number of taxa expected to benefit.
3. Multiply the two together, expressed as as $B_{total} = \sum p_{taxa} * \sum B_{base}$.

A future version may only sum the probabilities of taxa considered sensitive to variations in each component, which would require some reformulation. We currently lack comprehensive data to support such an approach, though Poff and Zimmerman (2010) provide a review on ecological responses to altered flow that could be used in addition to expert knowledge to build the required data.

3.3.3 Extending to multiple days and reaches

Once we have calculated the daily biologically-based benefit values for each segment, we can now perform annual, basinwide assessments. To obtain an annual basinwide value, simply sum all benefit values for each segment in the basin and day of the water year as in the equation in the objective function shown in Equation 2.1.

Alternative approaches could involve spatial connectedness of benefit values, reducing benefit for sets of segments with very low benefit that have higher benefit segments on each side. A situation like this with patches of high benefit could indicate that, while each location meets the needs of a species, the lack of contiguous high benefit segments could reduce the overall benefit. Migratory and resident fish would respond differently

to high benefit patches, requiring additional data on how fish use the streams (Adams, 2018; Adams et al., 2017).

3.4 Discussion

The method of calculating environmental benefit presented here has the benefit of requiring little information compared to other environmental flow models. Instead of calculating detailed and specific hydrologic information and relating it to species behavior, it takes an approach about restoration of historical processes that allows it to simplify the analysis to how well modeled flows match historical flows.

This method includes significant limitations, however. When historical flow data is unavailable or unreliable, some other way to quantify each functional flow is needed. More traditional environmental flow methods such as ecosystem and habitat modeling or expert judgment could fill the gaps.

Another limitation is in how the fuzzy components encourage variability in an optimization context. As currently constructed, they give an optimization model the ability to choose exact timing magnitude values for flows. But with large ranges of time and flow magnitude that all result in the same benefit value of 1, in the absence of other pressures, we might expect repeated years of model runs to result in similar functional flow regimes. Care should be exercised in interpreting results to focus on the trade-off curves as opposed to the specifics of the resulting optimal flow regime.

Finally, as noted early on, CEFF does not define single way to construct flow components from the modeled percentiles. The choices described in this chapter leave a large amount of natural variability out of the component entirely, or in the marginal "fuzzy" portion of the component. We chose values that seemed most appropriate for defining each component in an optimization context, but future work should include sensitivity analyses to understand the affect of these choices on the resulting trade-off curves.

3.5 Summary

This chapter discusses a simple method to assess the alignment of flows with their historical values to support the development and assessment of instream flow requirements. The method uses modeled historical flow data to construct a timing, duration, and magnitude box for a stream segment and flow component. Potential flows can be compared within that box to understand their alignment with historical flows and, by proxy, benefit to the ecosystem. We then scale the benefit, B_{base}, by the number of fish species we expect to be present to obtain B_{total} for a stream segment. In summing the values of B_{total} for all segments and days in a basin, we can assess the environmental value of flows in the system. The method assumes that alignment of flows provides environmental benefit on its own, which may not be true everywhere due to impairments in water quality or habitat. However, the simplifications in this method are designed to allow for widespread, rapid assessment of an entire basin, even in places without water quality data. The method allows for a rough valuation of environmental flows for use in further modeling.

Chapter 4

Estimating Trade-off Curves

4.1 Introduction

Chapter 3 detailed a method to quantify the value of a hydrograph to the ecosystem as a functional flow. This chapter applies that method in an optimization context along with a simplified economic demand curve for water. It uses an evolutionary algorithm to produce trade-off curve estimates for single stream segments or basins with objectives for environmental and economic benefit of flows based on chapter 3 and the objective functions in section 2.4.2. Trade-off curves have direct management relevance, including as information for a social process of setting environmental flow recommendations.

The model produced trade-off curves for many scenarios covering multiple water years and subsets of the Cosumnes River watershed. Computation time and model complexity prevented optimization of the entire watershed. The model is designed to be flexible and most pieces are data-driven and can be modified for each model run, allowing for future modifications that take advantage of the existing codebase even when applied to new watersheds. While this chapter's results are not immediately actionable for managers, they demonstrate the possibilities and provide a foundation to build on for a future model to more directly support management objectives by quantifying efficient trade-offs among objectives.

4.2 Methods

4.2.1 Site

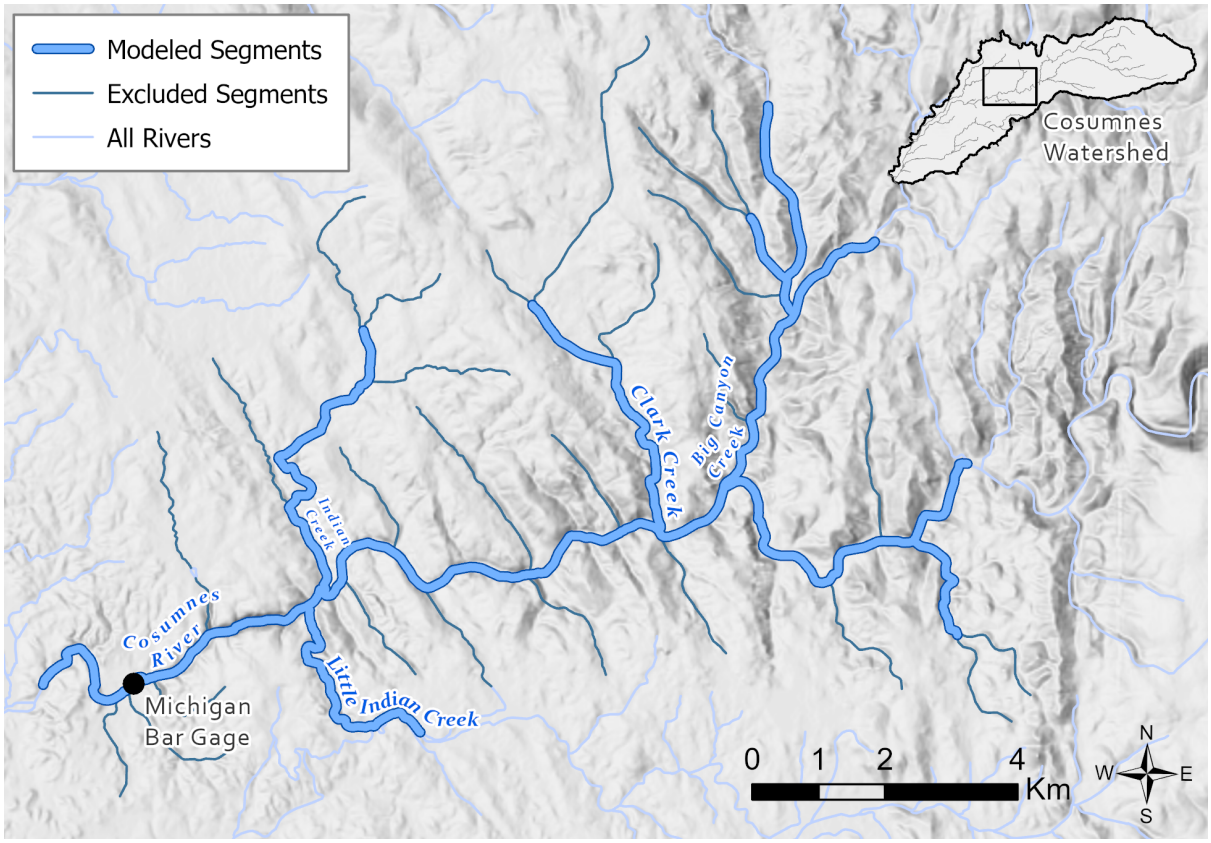

Figure 4.1 Map of the modeled portion of the Upper Cosumnes watershed. Thick segments in light blue are included in the model and thin dark segments were excluded because they lack sufficient flow metric data. Direction of flow is right to left on the mainstem Cosumnes.

The model optimized environmental flows on 43 National Hydrography Dataset stream segments in the Upper Cosumnes watershed (Watershed Boundary Dataset ID 1804001308). Four segments are downstream of the Michigan Bar USGS gage with the rest upstream. The selected site within the watershed had flow information from the Michigan Bar gage and available predicted flow metrics. The number of segments is constrained by computing power, with each function evaluation taking between 0.5 and 1 second to calculate the benefit of flows. Since the model requires millions of function evaluations to test and optimize, larger models are currently impractical but not infeasible.

The model includes two objective functions, as described in section 2.4.2. The decision variable is the proportion of flow to reserve for environmental uses for each stream segment and day included in the model. With 43 segments and 365 days in each water year, this is 15,695 decision variables. We ran the model separately for water years 2010 and 2011, moderate and wet water years, respectively, to assess performance for typical and high flows.

A linear demand curve (Equation 2.2) for water is based on the total amount of water demanded and an initial price of water, with the price of water reaching 0 when all

demand is satisfied. The total demand varies by water year and model run to explore the relationship between economic demand and environmental flows. We set the demanded amount of water at 80 percent of the most downstream segment's total annual runoff. The decision variables allow the model to change the segments and days to extract water to meet demand.

4.2.2 Interpolating Total Daily Flow

A primary input of the optimization model is daily flow data for each stream segment. Flow data are typically collected at stream gage sites, such as those from USGS, but the Upper Cosumnes watershed only has a single USGS stream gage at Michigan Bar (USGS ID 11335000). We used this gage to generate synthetic daily flows for every stream segment based both on the historical gage data and the California Unimpaired Flows Database, which provides modeled monthly data for every stream segment (Zimmerman et al., 2018). The USGS gage data provides high-resolution temporal variation in flows, while the Unimpaired Flows Database provides high-resolution spatial variation. Combined, we have a dataset that simulates how real flow events may have been distributed throughout the watershed.

To generate the daily flows, we first calculated a daily scaling factor for the gaged stream segment by dividing the actual flow measured by the gage by the modeled monthly flow from the Unimpaired Flows Database. We then applied the daily scaling factor to the monthly data for every stream segment to generate daily flows. For example, if the gaged segment had an estimated monthly flow of 200 CFS, but the gage showed a flow of 220 CFS for the day, then the scaling factor for that day, across the basin, would be $220/200 = 1.1$. Then, on another stream segment, if the modeled monthly flow was 21 CFS, the daily estimated flow was $21 * 1.1 = 23.1$ We applied this latter step to every stream segment in the basin.

Using these values directly would cause each unit of water to be counted more than once though, since we expect water in the upper segments to flow through all downstream segments in the same timestep. We calculated the contribution of the local watershed (Q_i) by subtracting water available upstream from the water available in the stream segment. If the amount upstream exceeds the total water available in a segment, the local contribution was set to 0.

4.2.3 Mass Balance in the Stream Network

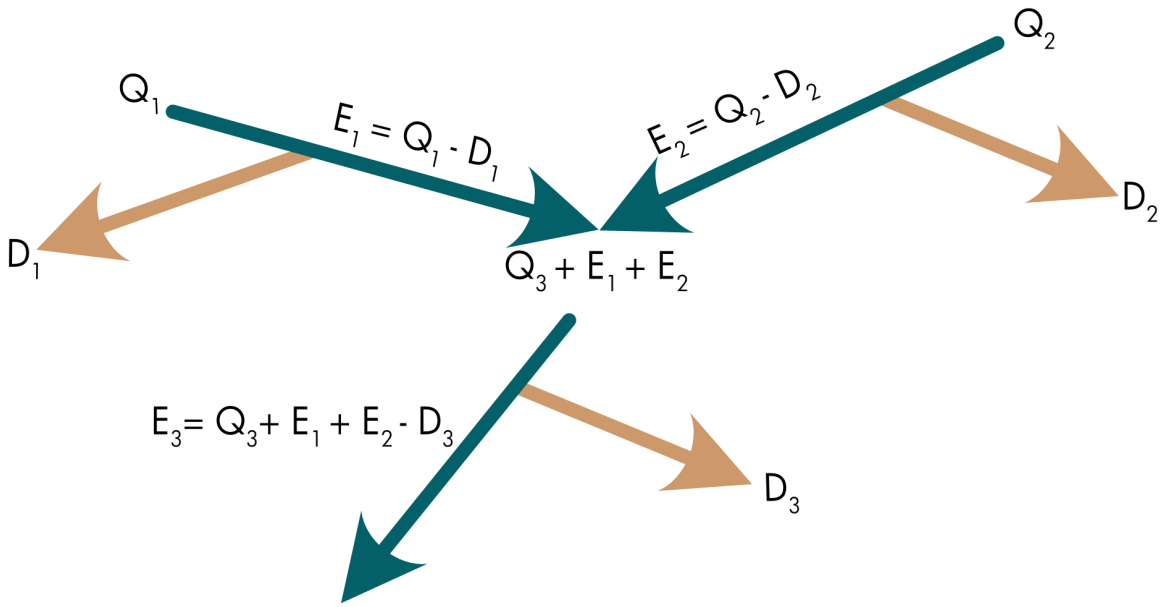

Figure 4.2 Water from each segment's local catchment (Q_i) and water allocated to environmental flows upstream are available to each segment for either economic or environmental allocation. Extracted water (D_i) is provided to the economic objective function and the remaining water (E_i) stays instream and is used to satisfy the environmental flow objective.

The model routes flows through an NHDPlus Version 2 stream network as shown in Figure 4.2. In each timestep it starts with the headwaters segments and continues downstream. The decision variables indicate the proportion of locally available water (Q_i + undiverted upstream flow) to remain instream as environmental flow (E_i) with the remaining water (D_i) extracted and passed to the economic objective function. Conceptually, each segment's point of diversion is at its top and water for economic purposes comes from a segment's total before the environmental flow calculation occurs. The environmental flow is available both for the segment's flow benefit and also to the downstream segment where it combines with the segment's locally contributed water as total available water to extract or use for environmental flows.

4.2.4 Software and Model Runs

This model was built and tested using Python 3.7.4 on Windows 10 and run on Ubuntu 18.04.3 virtual machines with Python 3.6.9 hosted in Microsoft Azure. It uses Django 3.0 and SQLite for data storage and management, and uses the Python package "Platypus" for running the evolutionary algorithms (Hadka, 2015). Full code for the model is on GitHub at https://github.com/ceff-tech/belleflopt/.

We ran the model with many parameter sets and algorithms to see if any one set was better for optimizing flows and also to get a qualitative sense of the model's sensitivity to specific inputs.

Model A. We ran every combination of model for each of the two water years (2010 and 2011), two population sizes (50 and 100), four random seeds (19991201, 18000408, 31915071, and 20200224), and four algorithms for 50,000 function executions (NFE) each. The algorithms used were the Nondominated Sorting Genetic Algorithm II (NSGAII), Generalized Differential Evolution 3 (GDE3), Strength Pareto Evolutionary Algorithm 2 (SPEA2), and Speed-constrainted Multiobjective Particle Swarm Optimization (SMPSO) algorithms (Deb et al., 2002; Kukkonen and Lampinen, 2005; Zitzler et al., 2001; Nebro et al., 2009). While the model does not converge in 50,000 NFE in any of these cases, we used it to explore which combinations might be likely to converge if run for more NFE and which algorithms might be used for more complete runs.

Model B. Based on the results in Model A, we ran both the 2010 and 2011 water years with the NSGAII and SPEA2 algorithms and a population size of 100 for 1,000,000 NFE each.

Model C. We ran both the 2010 and 2011 water years with NSGAII with a constraint on the lower limit on the proportion of a segment's flow assigned to the environment set at 0.75. We attempted this both to reduce the solution space to see if it would converge faster and also to prevent it from drawing all economic water from one or two segments as we might expect in the absence of such a constraint.

Model D. We ran a version that uses only 365 decision variables in the complete network. Each decision variable is the proportion of flow used for environmental flows, but the proportion is applied to every segment in the network.

Because performance considerations prevented these versions of the model from converging, we created another version (Model E) that used a single segment where the Michigan Bar gage is installed (NHD COMID 20192498). We ran it for both the 2010 and 2011 water years with four separate seeds each (34578239, 793539823, 912264360, and 20200224). The goal of this approach was to have the model run quickly enough on current hardware to converge and examine the resulting hydrographs.

We also ran the model to verify the approach of assigning benefit from flow components. We ran the model for one NFE with a fixed percentage of unimpaired flows allocated to environmental flows and calculated the benefit of those flows. We ran this for water years 2010 and 2011 for integer percentages from 0 to 100. If the approach is valid, benefit would increase as a larger percentage of flows are allocated to environmental flows.

4.3 Results

The verification run of the model resulted in a clear positive trend in the relationship between percentage of natural flow allocated to environmental flows and the estimated benefit. The results are shown in Appendix Figure C.1 for the full network and Figure C.2 for the Michigan Bar segment. The results for water year 2011 show a small decrease in benefit at the highest percentages of unimpaired flow, likely because four stream segments show unimpaired peak flows that exceed the 90^{th} percentile magnitude for the 2 year peak flow metric. While this method cannot fully test the model on its own, it suggests there are not glaring errors in the interpretation of flow components, the assignment of water to them, and the estimation of benefit from combining the two in the model.

Initial runs in Model A did not show signs of improvement indicating that they may eventually converge, even with weeks of computing time. The NSGAII and SPEA2 algorithms showed some improvement in the best options, leading to Model B where we ran each for 1,000,000 NFE with a population size of 100 for a total of 10,000 generations. That model was still slow to converge, though it showed some signs of improvement, so we experimented with reducing the search space by putting a lower limit on the proportion of flows dedicated to the environment (Model C) and with making a single decision variable for each day of the water year regardless of the segment (Model D). Model C was not appreciably faster per objective function evaluation, but improved more quickly. Model D did not appear to produce useful functional flow hydrographs, possibly due to the compounding effect of the withdrawal proportion as water flows through the network.

4.3.1 Michigan Bar Segment

Model E, which uses only the single Michigan Bar stream segment, converges on modern hardware within approximately 24 hours and 500,000 NFE for water year 2010. It shows the strengths and weaknesses of the environmental benefit calculations and produce trade-off curves for the single segment. The four random seeds produce similar trade-off curves. The model converges on environmental benefit first, then finds additional nondominated, but marginal, economic results with worse environmental benefit, extending the trade-off curve in the direction of lower environmental benefit. Resulting environmental benefit values for the best hydrographs ranged from 3057-3085 for water year 2010 and 3728-3754 for water year 2011.

Water year 2011, shown in Figure 4.3 included flows high enough to trigger evaluation of the peak component, resulting in higher overall environmental objective values. In Figure 4.3c, the model preserved some peak flows in accordance with the segment's flow metrics (see Table C.2 for a listing), but allowed water from other peak events to be extracted for economic use. Water year 2010, shown in Figure 4.4, had lower flows that did not activate the peak component. As a result, the model extracted most water, reducing environmental flows to baseflow, including existing small peak flows and leaving a small recession flow. It resulted in a deeply convex trade-off curve since, without peak flow benefit, the model could extract significant water for the economic objective without reducing the environmental objective.

The Pareto front in Figure 4.3d shows that even the best environmental result from the model includes most of the economic benefit (94 percent) since it allows for large amounts of water extraction while supporting a functional flow hydrograph. The Pareto front in Figure 4.4d indicates that the best environmental result has only about 80 percent of the

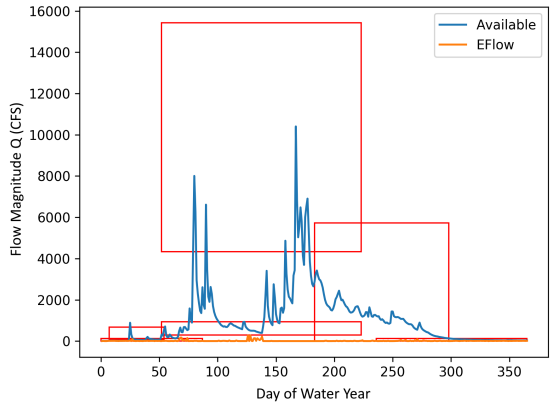

(a) Best economic benefit result (B=837)

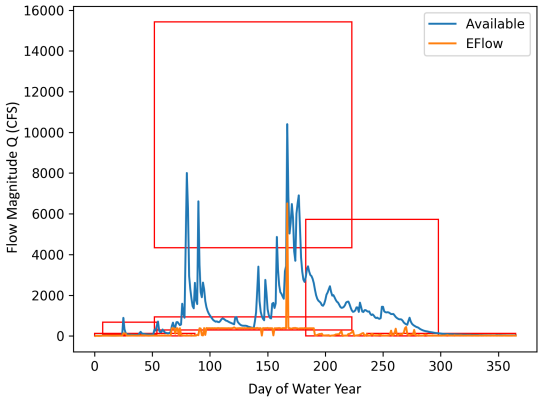

(b) Compromise result (B=3551)

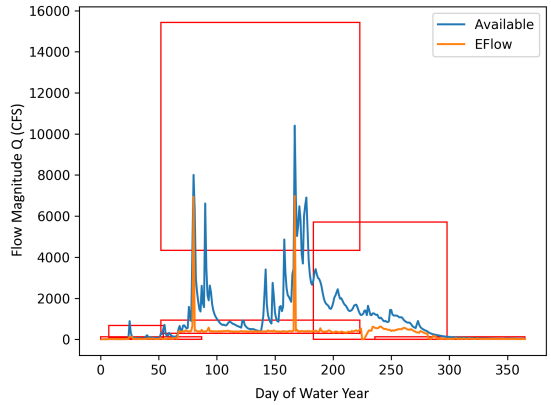

(c) Best environmental benefit result (B=3754)

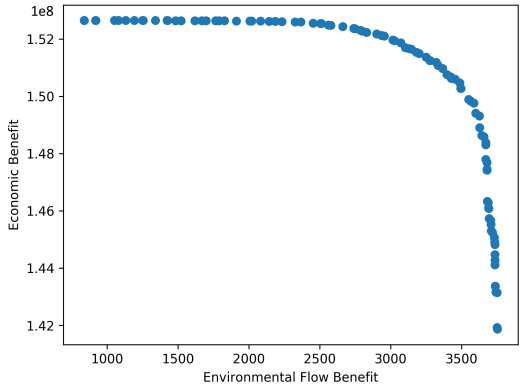

(d) Pareto front

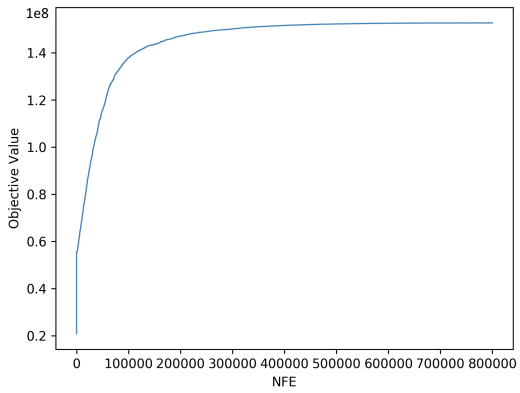

(e) Economic objective convergence curve

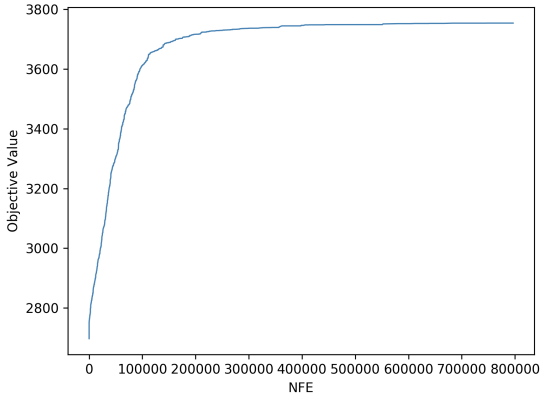

(f) Environmental objective convergence curve

Figure 4.3 Results of Model E for the Michigan Bar stream segment for water year 2011 with random seed 912264360. Red boxes on plots show outer bounds of constructed flow components. Convergence plots show best objective value encountered at each NFE. Full convergence plots are in Figure C.13 and Figure C.14.

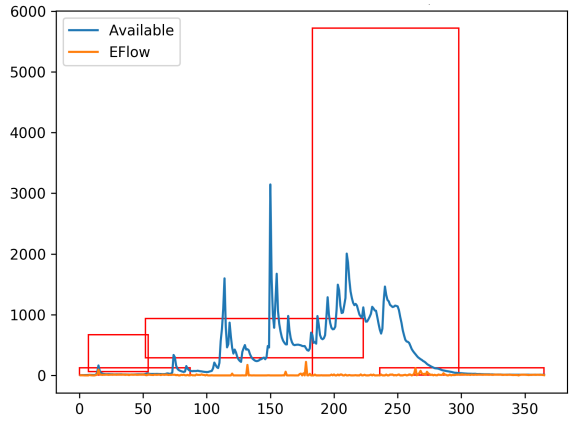

(a) Best economic benefit result

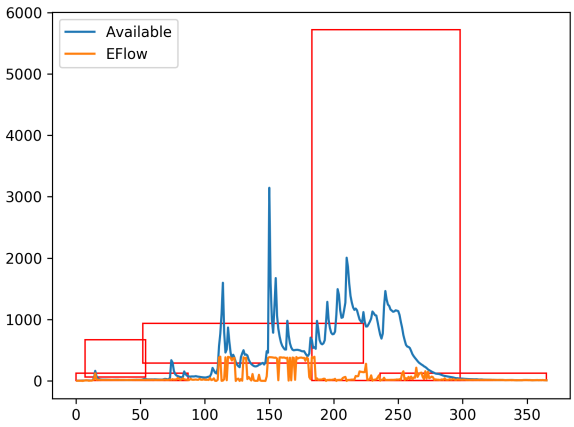

(b) Compromise result

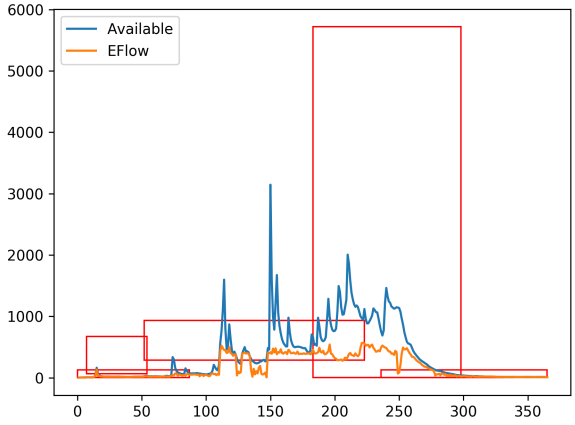

(c) Best environmental benefit result

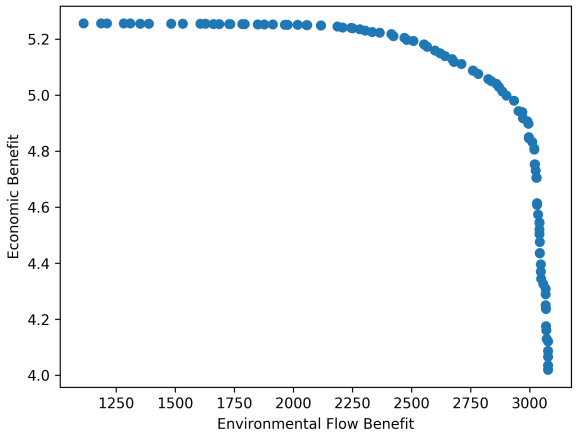

(d) Pareto front

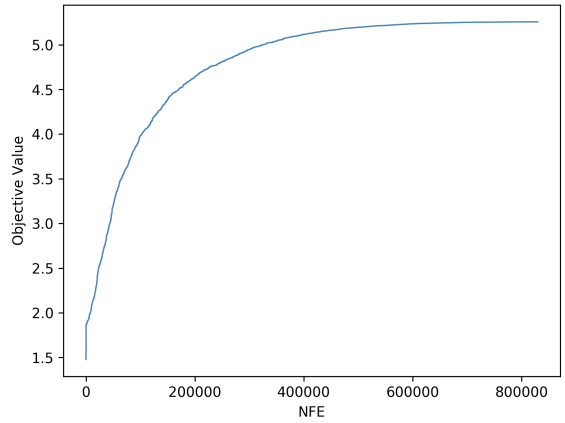

(e) Economic objective convergence curve

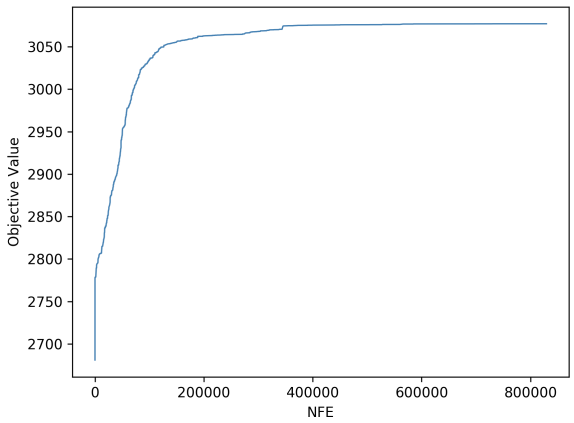

(f) Environmental objective convergence curve

Figure 4.4 Results of Model E for the Michigan Bar stream segment for water year 2010 with random seed 912264360. Red boxes on plots show outer bounds of flow components, except the peak component, which is not included here. Convergence plots show best objective value encountered at each NFE.

economic benefit from other results. The deep concavity of the trade-off curve suggests that strong compromise candidates might be available, but the compromise result in Figure 4.3b is qualitatively much worse, with only one peak flow, no spring recession, swings between winter baseflow and no flow, and a much earlier drop to baseflow in the summer.

4.4 Discussion

4.4.1 Model Performance

Though Model E's results for the Michigan Bar segment do not provide complete insight into basinwide environmental trade-offs, they show this approach's potential to optimize functional flow regimes and estimate their benefit. Even the single-segment model estimates the amount of water that can be extracted for economic purposes in a water year while maintaining a functional flow, which is a useful result on its own. The estimate for water extraction would likely change with more segments in the model though, so the result is incomplete.

With performance improvements, such as more efficient objective functions or better use of multicore computers, the model could be expanded to cover a larger connected network of stream segments as initially envisioned. Each water year converged in approximately 500,000 NFE, equivalent to around 24 hours of computing time for water year 2010 and 48 hours of computing time for water year 2011. All trade-off curves from every model version are concave, often deeply concave. Currently, we may lack enough detailed information in the economic model or in the flow model to create different shaped trade-off curves. Alternatively, the trade-off curves may be real representations that a concave relationship exists between the objectives in these locations.

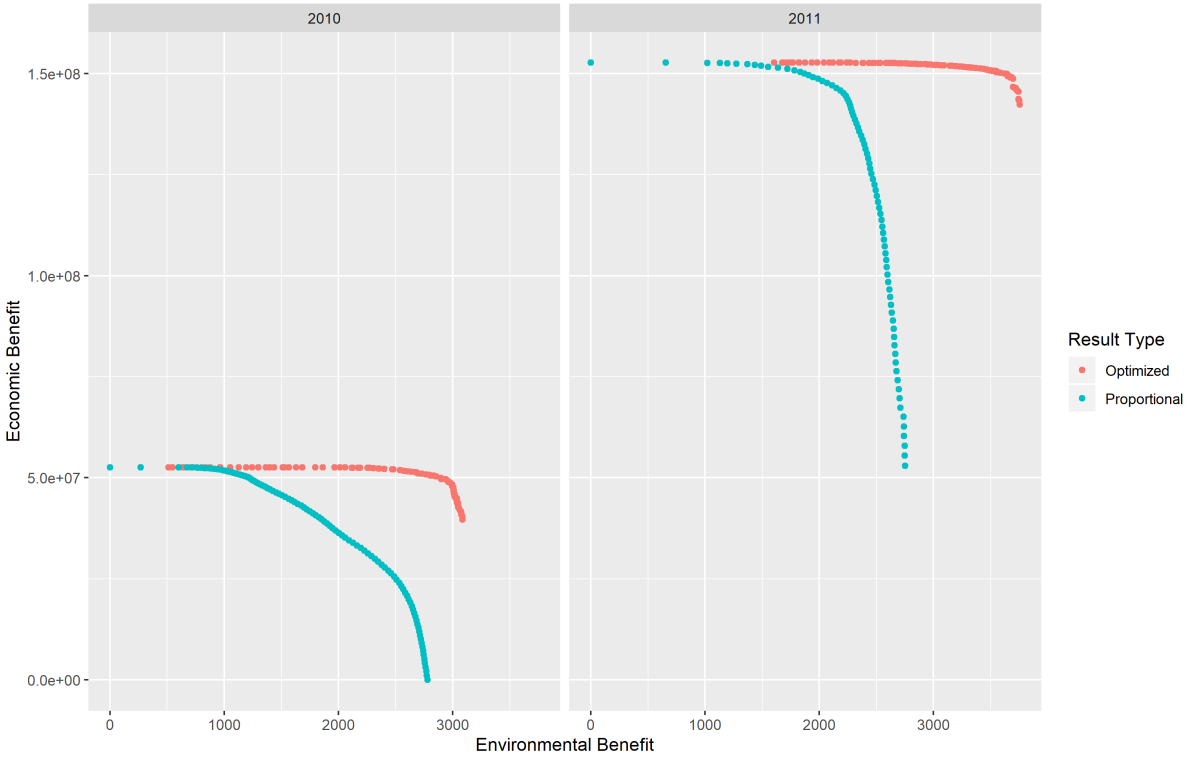

Figure 4.5 Final Pareto fronts (red) and curves showing the benefit of all days allocating the same fixed proportion of water to the environment (blue) with lower proportions in the top left and higher proportions in the top right. Larger versions of these plots are shown in Figure C.3 and Figure C.4.

In the results shown on Figure 4.3 and Figure 4.4, in both water years, the best environmental benefit (part c) may be the only viable solution, as a consequence of model design. While the economic objective can gain more benefit from extracting more water, nearly to the point of exhausting the system's water, the environmental objective includes concessions to the economic objective in the model design itself. By evaluating a functional flow, rather than a full natural flow, as the highest environmental benefit, the model allows for a large volume of extraction with no estimated losses to the environmental objective, shifting the trade-off curve. The flaw is visible in Figure 4.5, which shows the optimal Pareto fronts for model E with simple tradeoff curves generated from the proportional scaling used in the verification runs of the model. In an ideal case, the benefit values should match on those curves at their endpoints of all economic or all environmental flow. Between the endpoints though, the optimized results should improve relative to the naive proportional allocation since they can take water for economic uses at the least detrimental times.

Instead, the optimized results have a higher overall max benefit because the model only values functional flows, which in some cases means flows must be reduced to be valued. A more realistic approach may estimate high benefit for functional flows, but provide slightly more benefit to the environmental objective as it approaches the natural flow. Currently, the trade-off curve shows the consequences of degradation or alteration beyond a functional flow regime more than the full choices available to water managers in developing a functional flow regime.

4.4.2 Model Expansion

Currently, this model requires unimpaired flow data for each segment over an entire water year, limiting its use in impaired watersheds. To expand its use, modeled daily unimpaired flows would be needed, or other adjustments to the model to account for diversions and impoundments. Applying the model in one of these locations, provided data is available, also presents a new opportunity to adjust the demanded quantity of water to actual needs. We may also find use in adding additional flow information to the model such as floodplain activation thresholds and the associated ecosystem benefit, which could change the shape of the trade-off curves and better inform management.

Additionally, the economic objective function is highly simplified and assumes unlimited storage and free conveyance of water to the point of use. Since the model is likely to take all water from the most downstream segment, incorporation of pumping costs may encourage a more realistic spatial distribution of withdrawals. A more accurate model might treat the economic objective similarly to the environmental objective and build components from a demanded magnitude and timing of water. The difficulty is that, spatially, the point of use is often disconnected from the point of withdrawal, so we lack data to attach economic components to specific segments aside from water rights. Moving from a model-global water demand to localized demands may make the model more realistic, but also makes existing demands on the system a requirement, which may be helpful in some cases, but not in others.

4.4.3 Potential Adjustments

This problem's large set of decision variables made convergence difficult for traditional evolutionary algorithms. One possible reason is that individual changes in so many decision variables in a basin-scale model could cancel each other out when summed. The benefit estimated for any particular day might go up or down, but the individual effects cancel out so that the overall objective value does not change, even if some flow adjustments were very good. The problem may benefit from two pass optimization, where the first pass significantly narrows the solution space in a deterministic time-frame before initiating an algorithm such as NSGAII.

Another possible solution may be a windowed evaluation approach. By evaluating a fixed set of days, such as a week, on a single segment at a time, the model could reduce the chance that changes in decision variables will cancel each other out. If it evaluates each window many times and uses the results as an initial solution to an evolutionary algorithm, we may be able to increase the chance of convergence. Other possible ways to reduce the number of decision variable include using weekly decision variables and translate them to daily flows, use decision variables that represent different timeframes (eg: one decision variable covers all of summer baseflow, but winter peak component has many), or pre-narrowing the range of each decision values based on estimated benefit surfaces from chapter 3. The model appears more likely to converge in test runs with pre-narrowed ranges for decision values, though it is still slow and the method could be further refined.

As written, in some conditions, the model may undesirably alter flows without a corresponding decrease in environmental benefit. For example, in water year 2010, when flows were too low to activate the peak flow component, the best environmental flow regime the model produced stays close to the lower side of baseflow until the spring recession. In that case, the model sees the water above baseflow as essentially free. It can

take that water to increase the economic objective without decreasing the environmental objective, but at the expense of variation. When additional water is extracted at times or in volumes that may be environmentally detrimental, but the environmental objective does not return a lower value, then the shape of the trade-off curve will be distorted relative to how we would actually view that alteration. Future versions of the model should reconsider how to handle preserving some variability in years with flow magnitudes less than the peak flow component.

The model also struggles to handle the spring recession, possibly because of how the model estimates benefit for recession flows. Currently, for a small set of days, the model can get the most benefit by having a continuous decrease in flows for each day. But if the set of days increases to more than 14 days and then the model adjusts the environmental flow proportion, it is most likely to cause it to estimate 0 for the entire recession because of the penalty in the recession benefit functions. While the rules were set up to discourage large drops on any single day, they may also make it difficult for the model to find flow regimes with spring recessions. A future version of the model should rewrite the recession rules to make it easier for a random algorithm to create flow regimes that imitate recession flows while still discouraging large drops in flow. Another factor in the spring recession is that in cases where the recession component overlaps with the summer baseflow, the model may decide that it is just as optimal to drop to summer baseflow where it can get credit for summer baseflow and spring recession for the day. It then increases the flows and resumes a spring recession. A rapid drop in flow magnitude of this type is exactly what we wanted to avoid with the rules set up for recession benefit. The rules may need adjustment such as by increasing daily benefit for each subsequent recession day so that breaking a continuous streak of recession is disadvantageous.

Finally, the model's behavior when flows fall outside of flow components leads to undesirable choices. Currently, if natural flows drop below winter baseflow (e.g.: days 135-145 of water year 2010), the model decides to take all the daily flow for economic purposes, because there is no penalty for going lower. Results of this type add further evidence that the model needs to evaluate flows outside of components, possibly penalizing very low flows, even if it considers flows within the component boxes to be ideal.

4.5 Summary

The results show that the method described in this chapter can produce potential functional flow regimes in support of trade-off curve estimation. With future refinement to model environmental benefit calculations, model speed, and convergence performance, it could produce trade-off curves that support environmental flow decisions.

Chapter 5

Conclusions

This thesis proposed a model and reusable tool that optimizes environmental flows and water extractions for every stream segment in an entire basin, with a sample application in the Cosumnes River watershed in California. The optimization algorithm did not converge on a result for the larger networks of stream segments, but did converge for a single segment application, producing trade-off curves and potential functional flow regimes. Though the application has limited use in the Cosumnes watershed, it provides a demonstration for other watersheds. Additionally, the supporting work in estimating the environmental benefit of a functional flow regime may have use in CEFF processes as an extension to the work of Patterson et al. (In Review) in detecting hydrologic features.

5.1 Future Work

Future research for this model includes:

Validate species presence probabilities. The methods used to scale species data to stream segments should be validated by experts or external data. Other aquatic taxa beyond fish should be incorporated when possible.

Refining recession benefit calculations. Model results showed a spring recession only in ideal cases where the water year had a clear recession in the natural hydrograph. Only the best environmental results preserved the recession, despite its critical role in stream ecology. Further, the model fails to develop a spring recession in the more variable spring flows of water year 2011.

Improving model speed. Each function execution of the 41 segment model requires 1 second of CPU time on current hardware. An effective EA typically needs to run much faster, or have significant computing resources available, to run enough objective function executions to both converge the model and repeat it enough times to demonstrate a stable result. Performance optimization in the objective function make the model more valuable by increasing the ability to run the model to convergence and allowing us to run more model years or watersheds.

Benefit calculation changes. To provide a more complete picture of the tradeoffs in extracting water, the model needs to estimate benefit beyond when functional flows are met.

Algorithm changes to improve convergence. The larger models had difficulty converging, likely due to the number of decision variables. The model discussion notes potential solutions to increase the rate of convergence, including windowed evaluation, simplifications in the decision variables, reducing the available range of decision values (which showed potential in early testing), and two phase optimization.

With these improvements to the core model, further work would include additional code documentation and a web interface. Code documentation supports other researchers and managers in extending the model to support their use cases. The web interface would be designed for decision support, allowing managers without software development resources to provide parameters to the model and see resulting trade-off curves.

Appendices

Appendix A

Acknowledgements

Thanks first to the members of my committee and researchers at the Center for Watershed Sciences for their time, expertise, funding, input, and general support. Special thanks go to Drs. Jay Lund and Sarah Yarnell who guided me on grad school and the specifics of this project while being incredibly accessible and generous with their time. I feel very fortunate to have worked with two people who provide so much mentorship and support. Thanks also to my committee members, Jon Herman and Robert Hijmans, for their review of this thesis and also for their classes on evolutionary algorithms and spatial statistical methods.

My gratitude also goes to my spouse Kelly, my partner in life and writing. Without her understanding, emotional support, inspiration, discussion, and ideas of how to get out and do something fun sometimes, grad school would have been much harder.

Thanks also go to my supervisor and friend at the Center for Watershed Sciences, Dr. Cathryn Lawrence. I could not have asked for a better, more supportive mentor. Other staff and friends at the Center for Watershed Sciences have been incredibly important as well. Alyssa Obester and Dr. Ryan Peek provided my connection to the broader CEFF process, looping me in on information I needed to know and listening when I needed to talk a problem out. Matthew Chen wrote the first version of the code that downscaled PISCES species ranges. Drs. Josue Medellin-Azuara and Thomas Harter provided additional work for me and were incredibly understanding when I was slow on tasks while focused on school.

Additionally, thanks to Dr. Ted Grantham at UC Berkeley for his support in seeking funding for this project and Carrie Armstrong-Ruport, the UC Davis Geography Graduate Program Coordinator for all her help and support in the past few years.

Finally, thanks to the John Muir Institute for the Environment and the Center for Watershed Sciences for funding my time on this work and to Microsoft's AI for Earth program for providing cloud computing support used to run the model.

Appendix B

Code

Code for this project is available in the Git repository at https://github.com/ceff-tech/belleflopt. The code revision used was 0ad1adfb73af470cf6ab3a75a7a999648684f4b7.

Code to assign probabilities of species presence from PISCES data is available online in the Git repository at https://github.com/ceff-tech/ProbabilisticPISCES. The code revision used was 5be9c36f3a02f329346278c945a30bb47ab70946.

Appendix C

Additional Figures and Tables

Full sets of output plots for the versions of the model run for this document are available online at https://ucdavis.box.com/v/santos-thesis-eflows-opt.

C.0.1 Model Verification

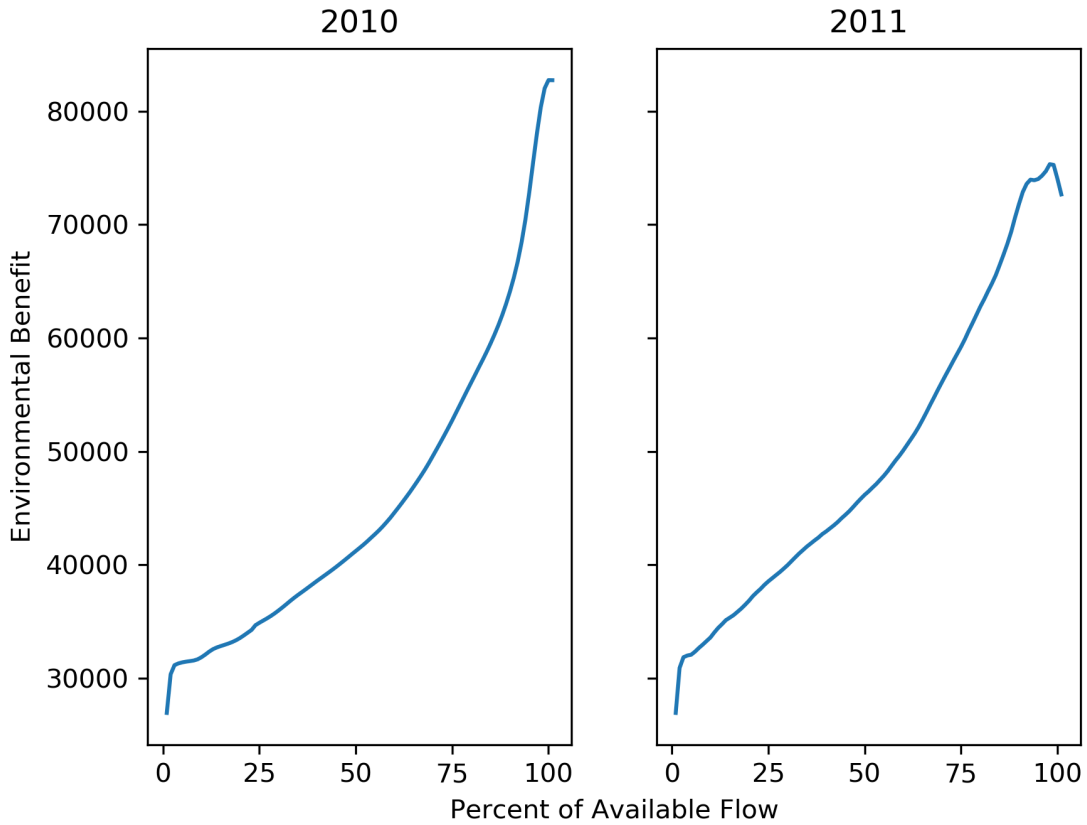

Figure C.1 Validation plot showing estimated benefit to set of 43 segments in study area with increasing percents of available flows allocated fo instream flow. Water year 2011 decreases in benefit at the highest flows because some unimpaired flow magnitudes exceed peak component maximum magnitude values.

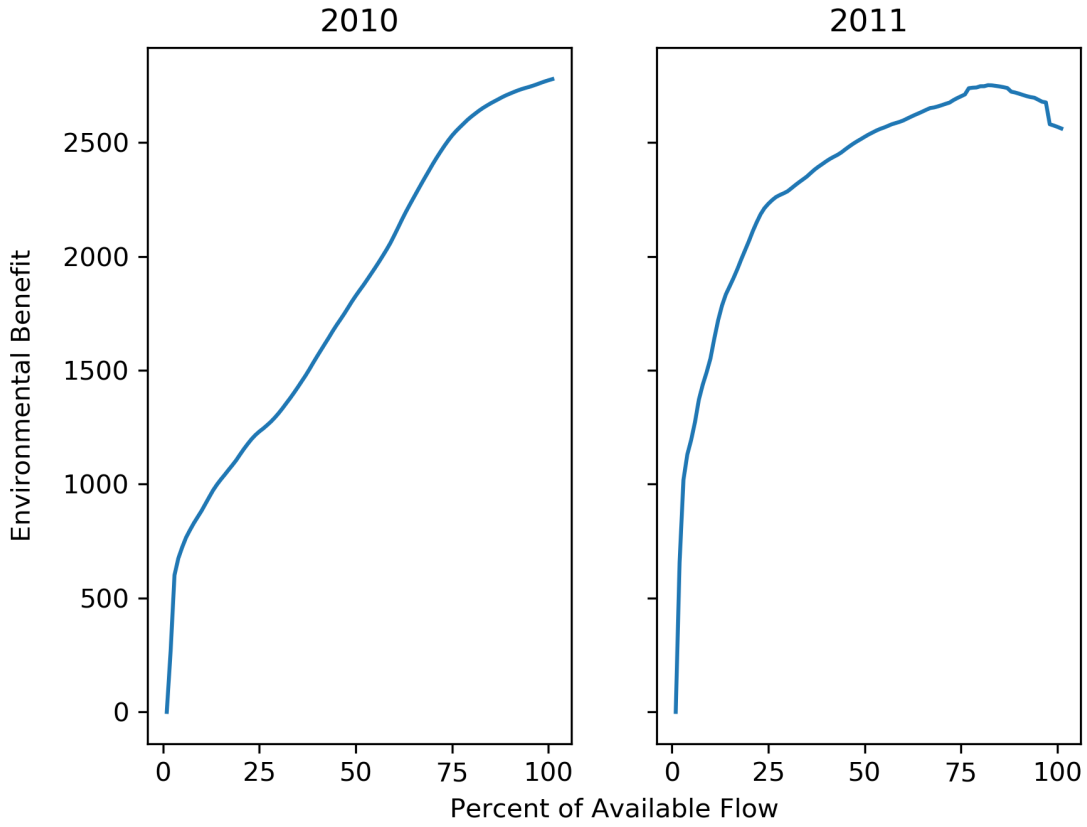

Figure C.2 Validation plot showing estimated benefit for the Michigan Bar stream segment with increasing percents of available flows allocated fo instream flow. Water year 2011 decreases in benefit at the highest flows because some flow magnitudes exceed peak component maximum magnitude values.

Proportional and Optimized 2010

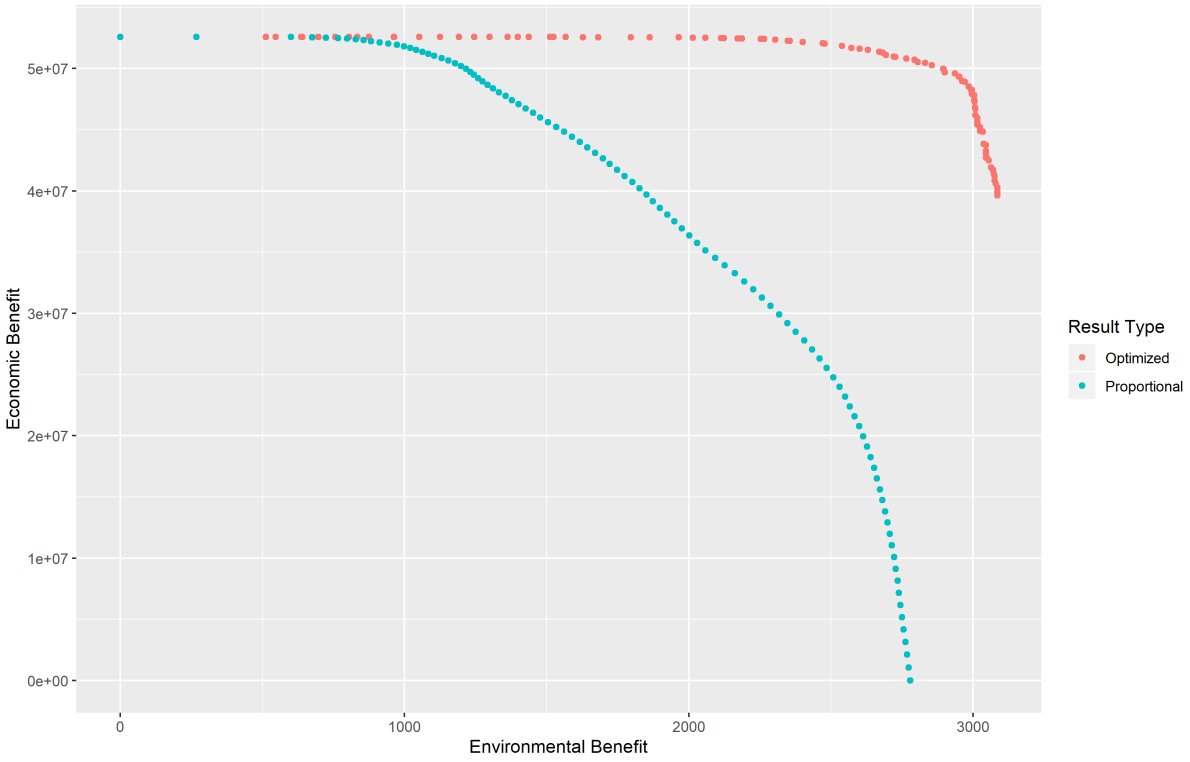

Figure C.3 Final 2010 Pareto front (red) and a curve for Model E showing the benefit of all days allocating the same fixed proportion of water to the environment (blue) with lower proportions in the top left and higher proportions in the top right.

Proportional and Optimized 2011

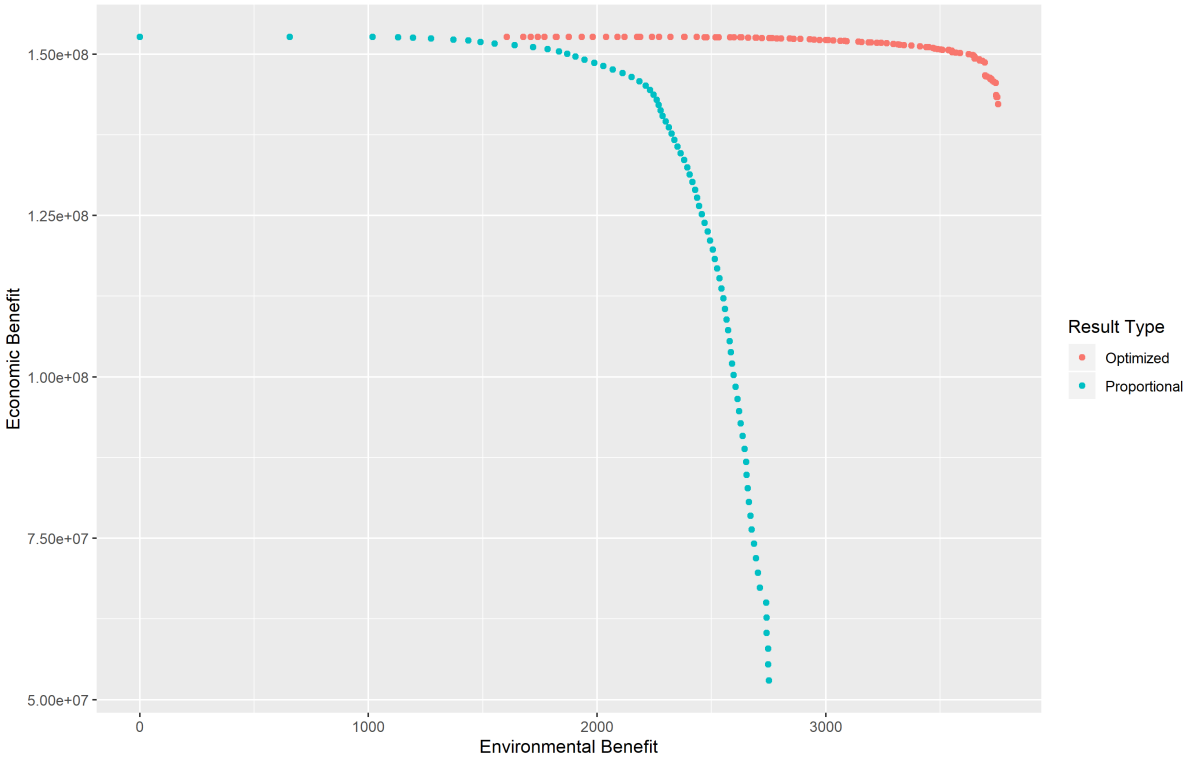

Figure C.4 Final 2011 Pareto front (red) and a curve for Model E showing the benefit of all days allocating the same fixed proportion of water to the environment (blue) with lower proportions in the top left and higher proportions in the top right.

C.0.2 Michigan Bar 2010 Results

All model runs here used a population size of 100 and the NSGAII algorithm and ran for 1,000,000 NFE. When the winter peak flow component box is not included in a graph, it is because in water year 2010, flows were not high enough to activate the peak component as it is built by the model.

Random Seed 20200224

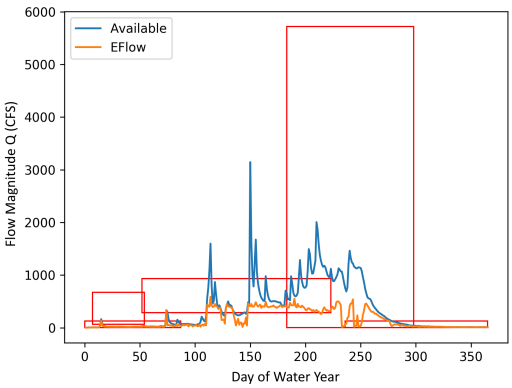

(a) Best environmental benefit result

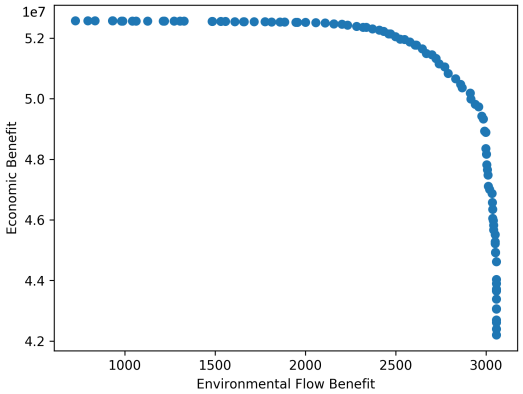

(b) Pareto front

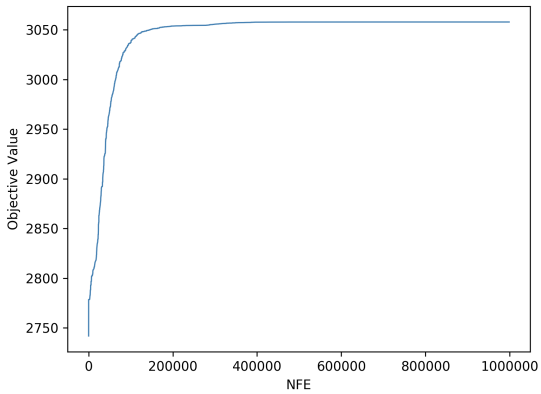

(c) Environmental convergence curve

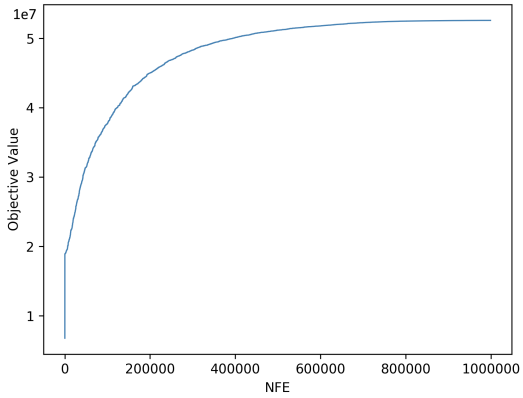

(d) Economic convergence curve

Figure C.5 Model E Results for Water Year 2010 with Random Seed 20200224. Best environmental benefit result was 3057 (unitless).

Random Seed 912264360

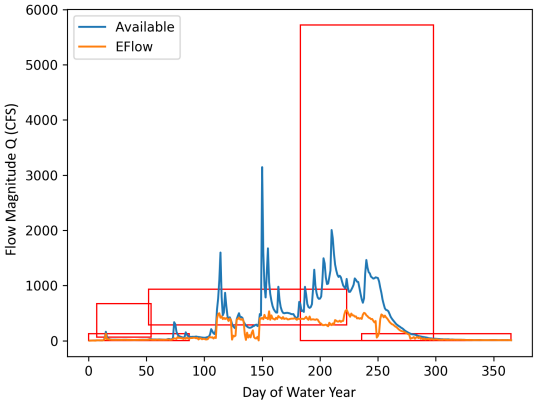

(a) Best environmental benefit result

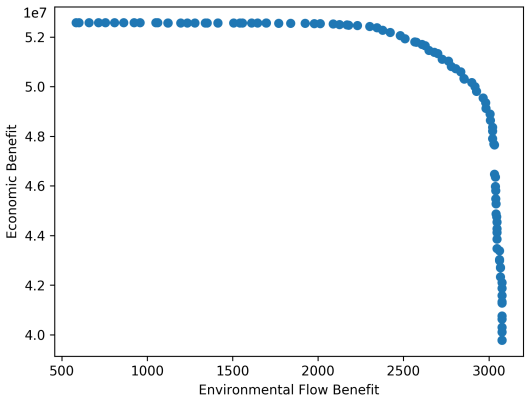

(b) Pareto front

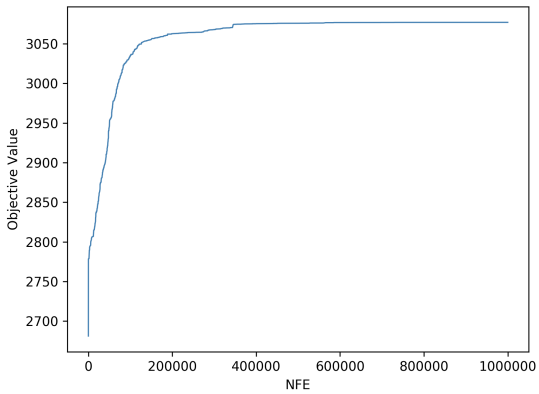

(c) Environmental convergence curve

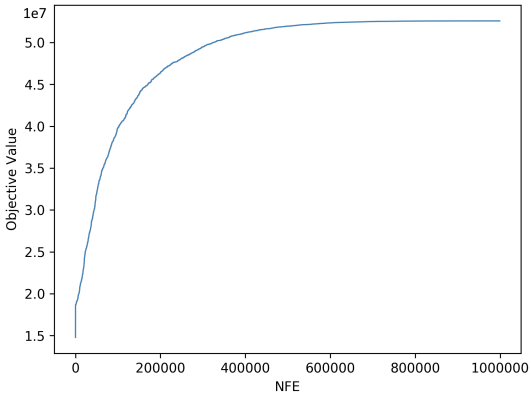

(d) Economic convergence curve

Figure C.6 Model E Results for Water Year 2010 with Random Seed 912264360. Best environmental benefit result was 3077 (unitless).

Random Seed 34578239

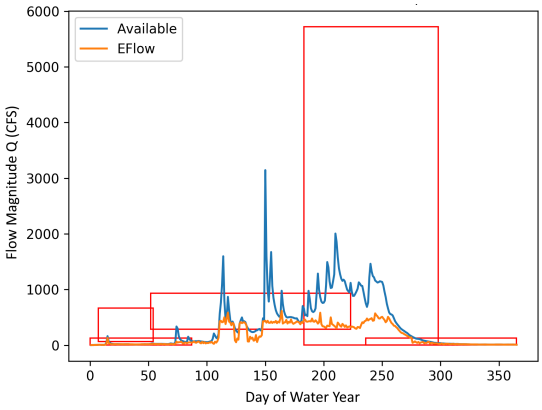

(a) Best environmental benefit result

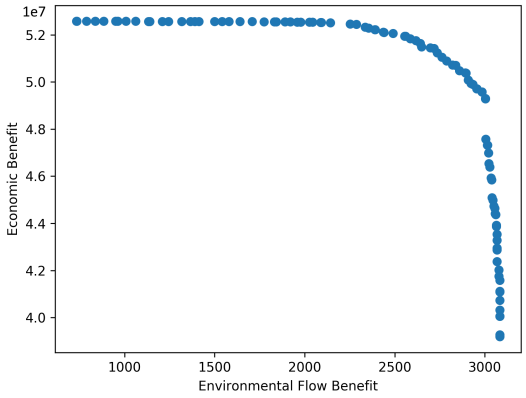

(b) Pareto front

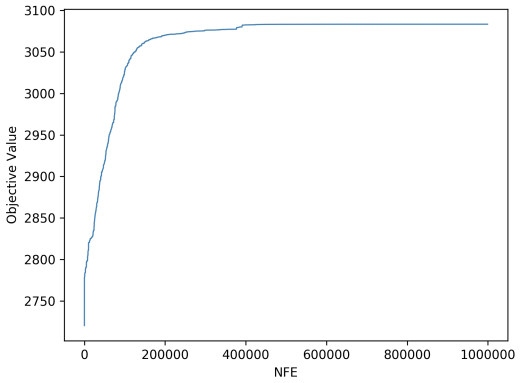

(c) Environmental convergence curve

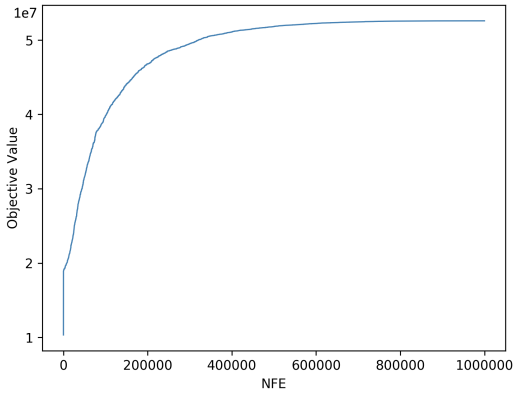

(d) Economic convergence curve

Figure C.7 Model E Results for Water Year 2010 with Random Seed 34578239. Best environmental benefit result was 3083 (unitless).

Random Seed 793539823

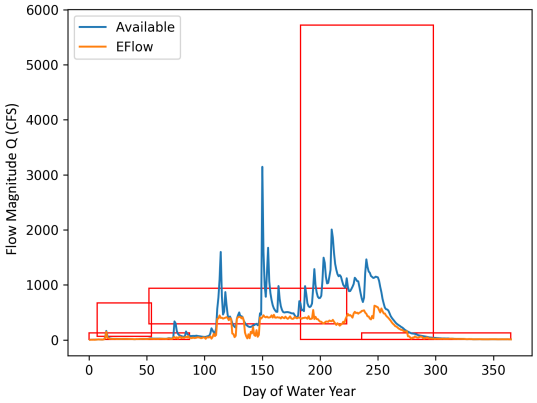

(a) Best environmental benefit result

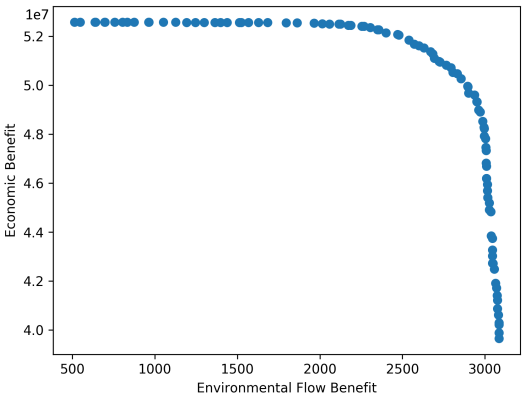

(b) Pareto front

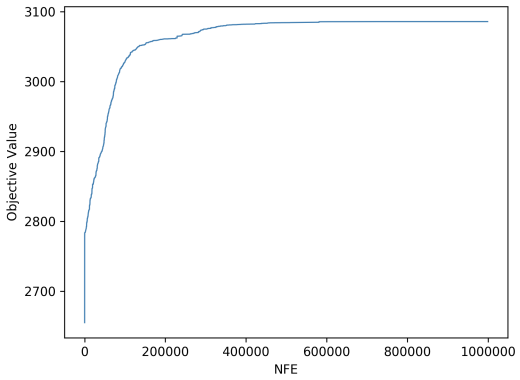

(c) Environmental convergence curve

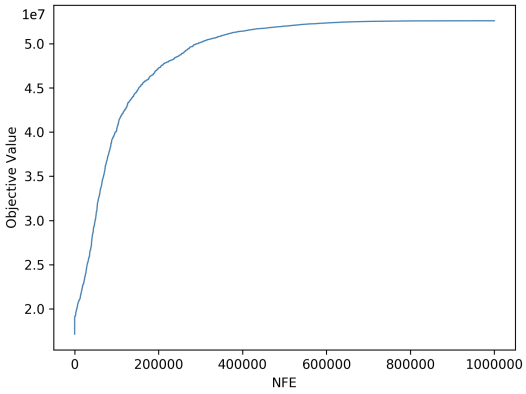

(d) Economic convergence curve

Figure C.8 Model E Results for Water Year 2010 with Random Seed 793539823. Best environmental benefit result was 3085 (unitless).

C.0.3 Michigan Bar 2011 Results

Random Seed 20200224

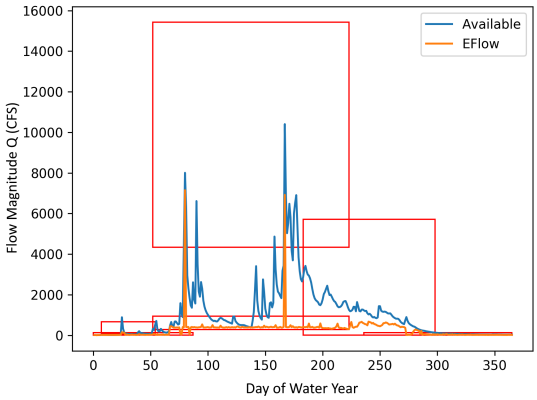

(a) Best environmental benefit result

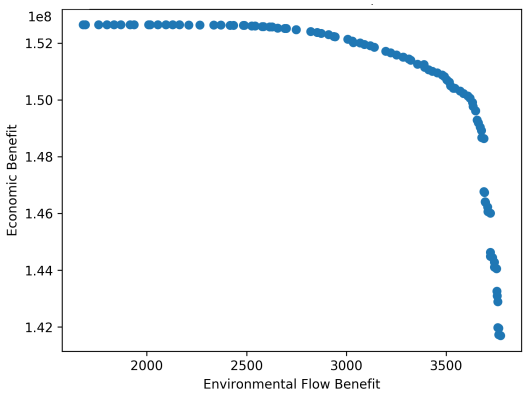

(b) Pareto front

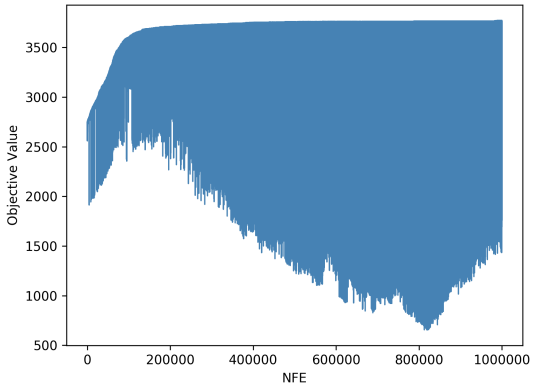

(c) Environmental convergence curve

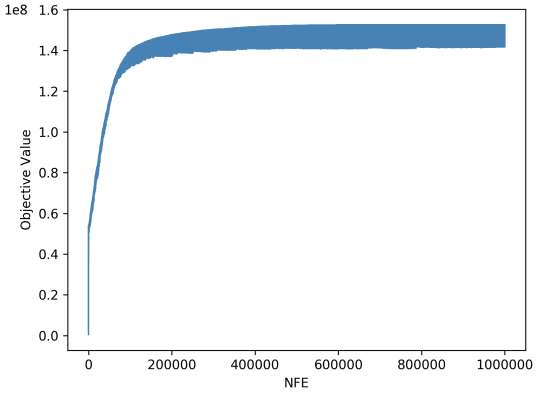

(d) Economic convergence curve

Figure C.9 Model E Results for Water Year 2011 with Random Seed 20200224. The model for this seed used older plotting code, resulting in plots that look different, though the underlying optimization code was equivalent. NFE=1,000,000 for this seed.

Random Seed 912264360

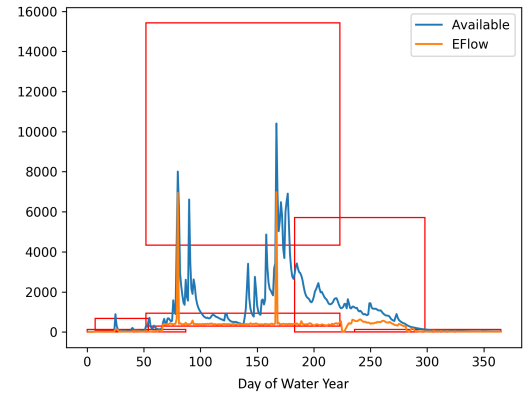

(a) Best environmental benefit result

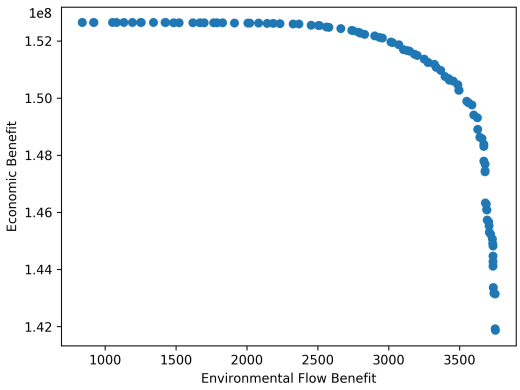

(b) Pareto front

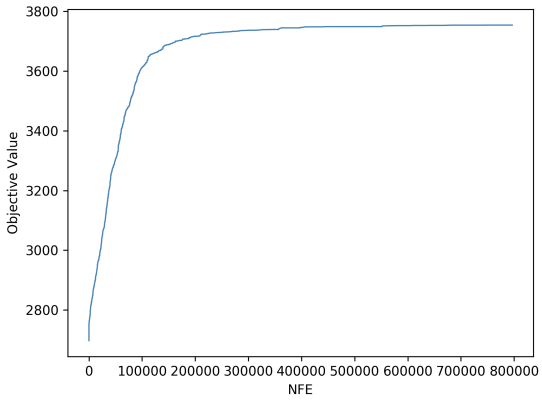

(c) Environmental convergence curve

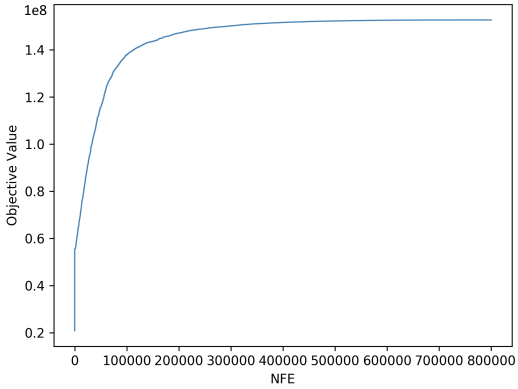

(d) Economic convergence curve

Figure C.10 Model E Results for Water Year 2011 with Random Seed 912264360. Best environmental benefit result was 3754 (unitless). NFE=800,000 for this seed.

Random Seed 34578239

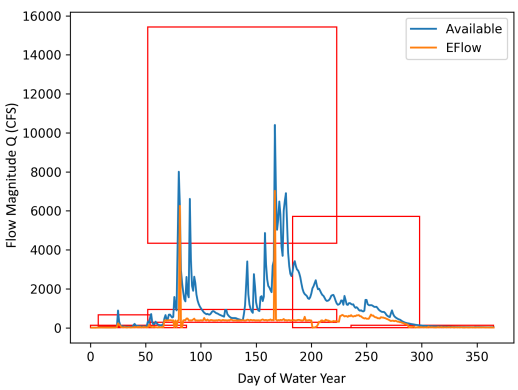

(a) Best environmental benefit result

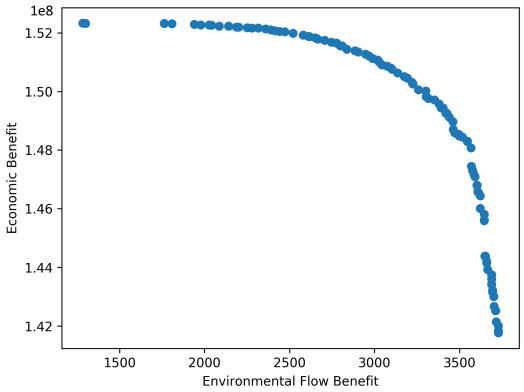

(b) Pareto front

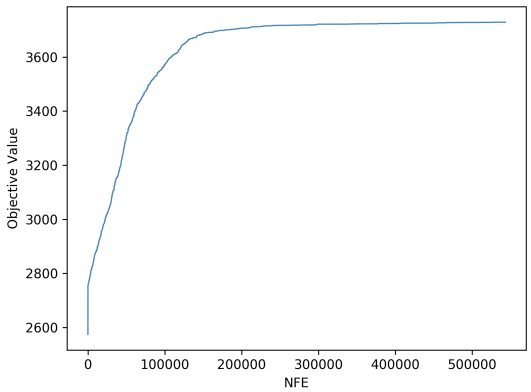

(c) Environmental convergence curve

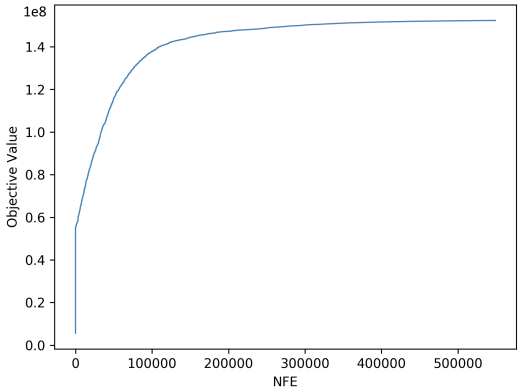

(d) Economic convergence curve

Figure C.11 Model E Results for Water Year 2011 with Random Seed 34578239. Best environmental benefit result was 3728 (unitless). NFE=550,000 for this seed.

Random Seed 793539823

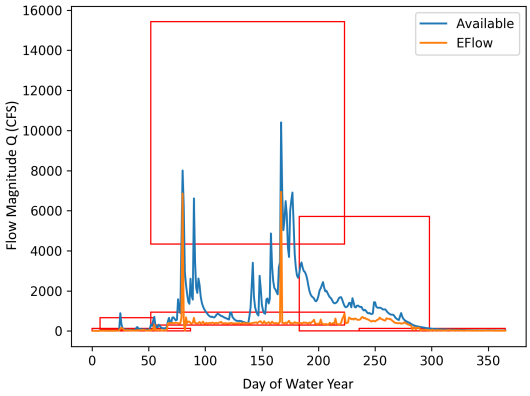

(a) Best environmental benefit result

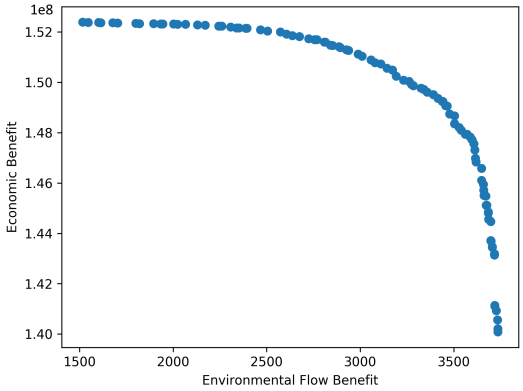

(b) Pareto front

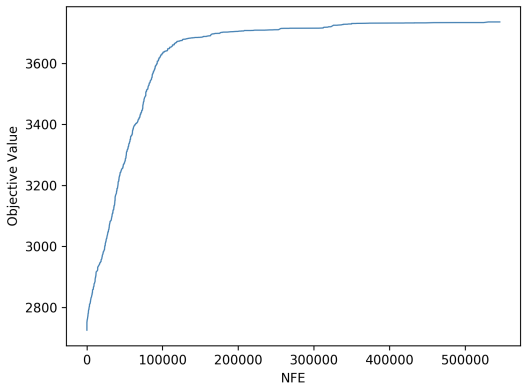

(c) Environmental convergence curve

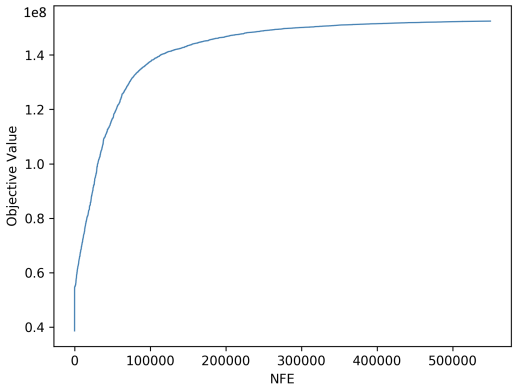

(d) Economic convergence curve

Figure C.12 Model E Results for Water Year 2011 with Random Seed 793539823. Best environmental benefit result was 3735 (unitless). NFE=550,000 for this seed.

Complete Convergence Curves

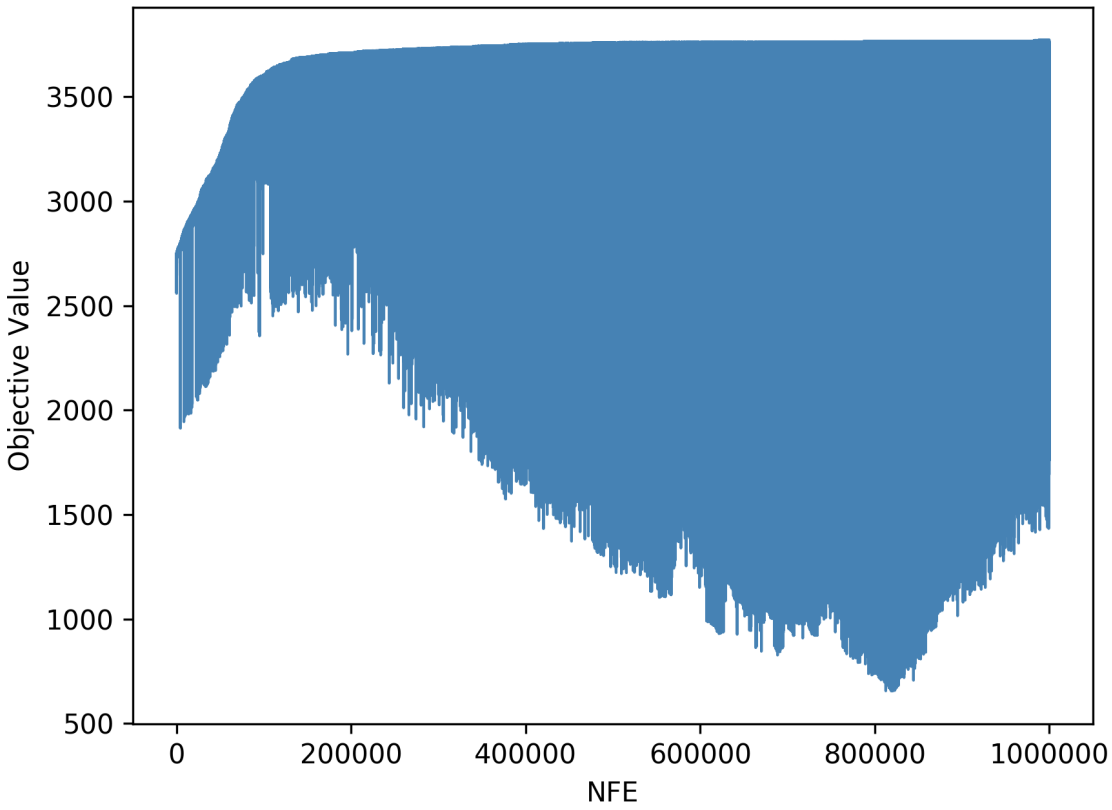

Figure C.13 Full Michigan Bar 2011 Environmental Objective Convergence for seed 20200224.

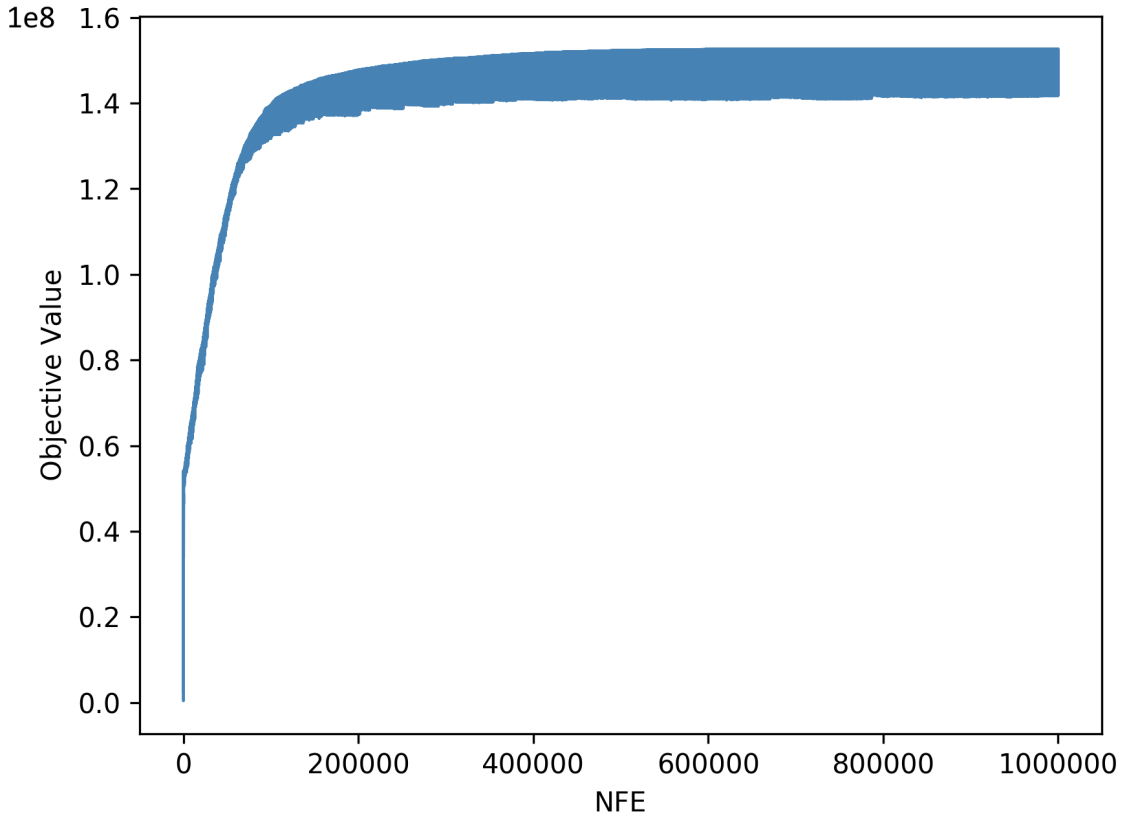

Figure C.14 Full Michigan Bar 2011 Economic Objective Convergence for seed 20200224.

C.0.4 Flow Metrics

Table C.1 Modeled flow metrics from Grantham et al. (in prep) used in the construction of the fuzzy benefit surfaces.

Component	CEFF Code	Magnitude Metric	Start Timing Metric	Duration Metric
Dry-season base flow	DS	DS_Mag_50	DS_Tim	DS_Dur_WS
Wet-season base flow	Wet_BFL	Wet_BFL _Mag_50	Wet_Tim	Wet_BFL _Dur
Wet-season peak flow	Peak	Peak_20	Wet_Tim	Peak_Dur_20
Fall pulse flow	FA	FA_Mag	FA_Tim	FA_Dur
Spring recession flow	SP	SP_Mag	SP_Tim	SP_Dur

In addition to the metrics in Table C.1, we also use Peak_Fre_20 as the peak frequency metric and SP_ROC as the spring recession rate of change metric. For fall pulse flow, we do not use a frequency metric because we assume only a single peak event for the flushing flow (CEFF Contract Team, 2020).

C.0.5 Michigan Bar Flow Metric Values

Table C.2 Modeled CEFF flow metrics values from Grantham et al. (in prep) used to construct the fuzzy flow metric surfaces for the Michigan Bar stream segment, COMID 20192498. Flow metrics marked with asterisks were not used in the model.

Flow Metric	p10	p25	p50	p75	p90
DS_Dur_ws	109.24	134.60	160.85	185.87	216.8
DS_Mag_50	6.68	15.21	34.93	71.66	126.61
DS_Mag_90	39.66	60.78	100.28	146.14	227.17
DS_Tim	236.14	255.62	268.95	285.72	303.91
FA_Dur	2	3	4	7	9
FA_Mag	64.80	117.26	212.30	366.33	670.70
FA_Tim	7.73	14	27.12	38.36	47.63
Peak_2	4334.80	6848.01	7639.14	10938.52	15425.46
Peak_5*	10779.49	12610.50	13731.42	19552.86	23449.10
Peak_10*	15779.05	18672.20	18814.76	20989.90	25919.84
Peak_Dur_2	1	1	3	7	16
Peak_Dur_5*	1	1	1	3	4.8
Peak_Dur_10*	1	1	1	2	3.2
Peak_Fre_2	1	1	2	3	5
Peak_Fre_5*	1	1	1	2	3
Peak_Fre_10*	1	1	1	1	2
SP_Dur	32.88	44.26	60.31	85.65	115.06
SP_Mag	667.77	1078.90	1953.72	3332.53	5718.93
SP_ROC	0.04	0.05	0.07	0.10	0.16
SP_Tim	167.67	183.5	199.68	212	228.01
Wet_BFL_Dur	71.73	95	121.11	147.06	171.18
Wet_BFL_Mag_50	290.42	376.22	510.00	688.33	936.90
Wet_BFL_Mag_10*	66.41	104.15	182.89	252.36	343.59
Wet_Tim	52.11	64.68	76.82	89.72	102.60

C.0.6 Species Presence from PISCES

Table C.3 Species present on modeled Cosumnes River stream segments and their probability of occurrence at the Michigan Bar segment. The Michigan Bar segment has all of the species present in other segments, though presence probabilities may vary in other segments. Data pulled from PISCES on October 22, 2019 and available online at https://github.com/ceff-tech/ProbabilisticPISCES/releases.

Common Name	Scientific Name	PISCES Species Code	Probability
Inland threespine stickleback	Gasterosteus aculeatus microcephalus	GGA02	1
Western brook lamprey	Lampetra richardsoni	PLR01	1
Sacramento sucker	Catostomus occidentalis occidentalis	CCO01	1
Coastal rainbow trout	Oncorhynchus mykiss irideus	SOM09	1
Prickly sculpin	Cottus asper	CCA02	1
Sacramento pikeminnow	Ptychocheilus grandis	CPG01	1
Riffle sculpin	Cottus gulosus	CCG01	1
California roach	Hesperoleucus symmetricus symmetricus	CLS01	1
Sacramento blackfish	Orthodon microlepidotus	COM01	1
Sacramento hitch	Lavinia exilicauda exilicauda	CLE01	1

C.0.7 Primary Stream Orders

Table C.4 Calculated primary stream order for all taxa in PISCES marked as "wide ranging". Data pulled from PISCES on October 22, 2019 and available online at https://github.com/ceff-tech/ProbabilisticPISCES/releases.

Common Name	Scientific Name	PISCES Species Code	Primary Stream Order
Klamath smallscale sucker	Catostomus rimiculus	CCR01	2
Lahontan speckled dace	Rhinichthys osculus robustus	CRO02	1
Sacramento speckled dace	Rhinichthys osculus subspecies	CRO01	1
Coastal threespine stickleback	Gasterosteus aculeatus aculeatus	GGA01	1
Pit River tui chub	Siphatales thalassinus subspecies	CST02	2
Klamath River lamprey	Entosphenus similis	PES01	2
Lahontan redside	Richardsonius egregius	CRE01	1
Delta smelt	Hypomesus pacificus	OHP01	1
Shortnose sucker	Chasmistes brevirostris	CCB01	1
Lower Klamath marbled sculpin	Cottus klamathensis polyporus	CCK02	2
Paiute sculpin	Cottus beldingi	CCB02	1
Inland threespine stickleback	Gasterosteus aculeatus microcephalus	GGA02	1
Lost River sucker	Catostomus luxatus	CCL01	1
Mountain whitefish	Prosopium williamsoni	SPW01	1
Arroyo chub	Gila orcutti	CGO01	1
Northern tidewater goby	Eucyclogobius newberryi	GEN01	1
Desert pupfish	Cyprinodon macularius	CCM02	1
Western brook lamprey	Lampetra richardsoni	PLR01	1
Sacramento pikeminnow	Ptychocheilus grandis	CPG01	1
Southern coastal roach	Hesperoleucus venustus subditus	CLS05	1
Southern tidewater goby	Eucyclogobius kristinae	GEK01	2
Humboldt sucker	Catostomus occidentalis humboldtianus	CCO04	2
Staghorn sculpin	Leptocottus armatus	CLA01	1
Razorback sucker	Xyrauchen texanus	CXT01	2
Pit-Klamath brook lamprey	Lampetra lethophaga	PLL01	2
Sacramento sucker	Catostomus occidentalis occidentalis	CCO01	1
Tahoe sucker	Catostomus tahoensis	CCT01	1
Monterey sucker	Catostomus occidentalis mnioltiltus	CCO03	2
Coastal rainbow trout	Oncorhynchus mykiss irideus	SOM09	1
Riffle sculpin	Cottus gulosus	CCG01	1
Klamath speckled dace	Rhinichthys osculus klamathensis	CRO03	1

Common Name	Scientific Name	PISCES Species Code	Primary Stream Order
Lahontan stream tui chub	Siphatales bicolor obesus	CSB04	2
Starry flounder	Platichthys stellatus	PPS01	1
Sacramento splittail	Pogonichthys macrolepidotus	CPM01	1
California roach	Hesperoleucus symmetricus symmetricus	CLS01	1
Northern coastal roach	Hesperoleucus venustus navarroensis	CLS03	3
Lahontan cutthroat trout	Oncorhynchus clarki henshawi	SOC03	1
Owens sucker	Catostomus fumeiventris	CCF01	2
California killifish	Fundulus parvipinnis	CFP01	1
Striped mullet	Mugil cephalus	MMC02	1
Hardhead	Mylopharodon conocephalus	CMC01	1
Sacramento tule perch	Hysterocarpus traskii traskii	EHT01	1
Sacramento perch	Archoplites interruptus	CAI01	1
Prickly sculpin	Cottus asper subspecies	CCA02	1
Klamath largescale sucker	Catostomus snyderi	CCS01	1
Santa Ana sucker	Catostomus santaanae	CCS02	3
Sacramento blackfish	Orthodon microlepidotus	COM01	1
Coastrange sculpin	Cottus aleuticus	CCA04	1
Kern brook lamprey	Lampetra hubbsi	PLH01	3
Pit sculpin	Cottus pitensis	CCP02	1
Lahontan mountain sucker	Pantosteus lahontan	CCP01	1
Monterey hitch	Lavinia exilicauda harengeus	CLE03	2
Sacramento hitch	Lavinia exilicauda exilicauda	CLE01	1

References

Adams, L. E., J. R. Lund, P. B. Moyle, R. M. Quiñones, J. D. Herman, and T. A. O'Rear (2017). "Environmental Hedging: A Theory and Method for Reconciling Reservoir Operations for Downstream Ecology and Water Supply". In: *Water Resources Research*, pp. 1–16. ISSN: 00431397. DOI: 10.1002/2016WR020128.

Adams, Lauren (2018). "Optimized Reservoir Management for Downstream Environmental Purposes". en. PhD thesis. University of California, Davis.

Ahmadi-Nedushan, B., A. St-Hilaire, M. Bérubé, T. B. M. J. Ouarda, and É Robichaud (2008). "Instream Flow Determination Using a Multiple Input Fuzzy-Based Rule System: A Case Study". en. In: *River Research and Applications* 24.3, pp. 279–292. ISSN: 1535-1467. DOI: 10.1002/rra.1059.

Arthington, Angela H. (2012). *Environmental Flows: Saving Rivers in the Third Millenium*. University of California Press. ISBN: 978-0-520-26910-1.

California Natural Resources Agency, California Environmental Protection Agency, and California Department of Food and Agriculture (2020). *California 2020 Water Resilience Porfolio*. Tech. rep., p. 148.

CEFF Contract Team (2020). *California Environmental Flows Framework - Guidance Document*.

Chart, Tom, Gary Burton, Dave Irving, Kirk LaGory, Robert Muth, Heather Patno, Dave Speas, and Richard Valdez (Feb. 2007). *Study Plan for the Implementation and Evaluation of Flow and Temperature Recommendations for Endangered Fishes in the Green River Downstream of Flaming Gorge Dam*. Tech. rep. Green River Study Plan Ad hoc Committee, p. 84.

Corporation, Horizon Systems (2018). "NHDPlus Version 2". In:

Deb, K., A. Pratap, S. Agarwal, and T. Meyarivan (Apr. 2002). "A Fast and Elitist Multiobjective Genetic Algorithm: NSGA-II". In: *IEEE Transactions on Evolutionary Computation* 6.2, pp. 182–197. ISSN: 1089-778X. DOI: 10.1109/4235.996017.

Dogan, Mustafa S., Max A. Fefer, Jonathan D. Herman, Quinn J. Hart, Justin R. Merz, Josue Medellín-Azuara, and Jay R. Lund (Oct. 2018). "An Open-Source Python Implementation of California's Hydroeconomic Optimization Model". en. In: *Environmental Modelling & Software* 108, pp. 8–13. ISSN: 1364-8152. DOI: 10.1016/j.envsoft.2018.07.002.

Draper, Andrew J., Marion W. Jenkins, Kenneth W. Kirby, Jay R. Lund, and Richard E. Howitt (May 2003). "Economic-Engineering Optimization for California Water Management". en. In: *Journal of Water Resources Planning and Management* 129.3, pp. 155–164. ISSN: 0733-9496, 1943-5452. DOI: 10.1061/(ASCE)0733-9496(2003)129:3(155).

Dudgeon, David, Angela H. Arthington, Mark O. Gessner, Zen-Ichiro Kawabata, Duncan J. Knowler, Christian Lévêque, Robert J. Naiman, Anne-Hélène Prieur-Richard, Doris Soto, Melanie L. J. Stiassny, and Caroline A. Sullivan (May 2006). "Freshwa-

ter Biodiversity: Importance, Threats, Status and Conservation Challenges". en. In: *Biological Reviews* 81.2, pp. 163–182. ISSN: 1469-185X, 1464-7931. DOI: 10.1017/S1464793105006950.

Grantham, Theodore, Kirk Klausmeyer, and Julie Zimmerman (in prep). *Functional Flow Metric Modeling*. Tech. rep.

Hadka, David (2015). *Platypus - Multiobjective Optimization in Python*.

Homa, Vogel R. M., Smith M. P., Apse C. D., Huber-Lee A., and Sieber J. (2005). "An Optimization Approach for Balancing Human and Ecological Flow Needs". In: *Impacts of Global Climate Change*. Proceedings. ISSN: 9780784407929. DOI: 10.1061/40792(173)76.

Horne, Avril, Joanna M. Szemis, Simranjit Kaur, J. Angus Webb, Michael J. Stewardson, Alysson Costa, and Natashia Boland (Oct. 2016). "Optimization Tools for Environmental Water Decisions: A Review of Strengths, Weaknesses, and Opportunities to Improve Adoption". In: *Environmental Modelling & Software* 84, pp. 326–338. ISSN: 1364-8152. DOI: 10.1016/j.envsoft.2016.06.028.

Howard, Jeanette K, Kirk R Klausmeyer, Kurt A Fesenmyer, Joseph Furnish, Thomas Gardali, Ted Grantham, Jacob V E Katz, Sarah Kupferberg, Patrick McIntyre, Peter B Moyle, Peter R Ode, Ryan Peek, Rebecca M Quiñones, Andrew C Rehn, Nick Santos, Steve Schoenig, Larry Serpa, Jackson D Shedd, Joe Slusark, Joshua H Viers, Amber Wright, and Scott A Morrison (2015). "Patterns of Freshwater Species Richness, Endemism, and Vulnerability in California." English. In: *PLoS ONE* 10.7, e0130710. DOI: 10.1371/journal.pone.0130710.

Jager, Henriette I. and Kenneth A. Rose (Feb. 2003). "Designing Optimal Flow Patterns for Fall Chinook Salmon in a Central Valley, California, River". In: *North American Journal of Fisheries Management* 23.1, pp. 1–21. ISSN: 0275-5947. DOI: 10.1577/1548-8675(2003)023⟨0001:DOFPFF⟩2.0.CO;2.

Jorde, Klaus, Matthias Schneider, Armin Peter, and Frank Zoellner (2001). "Fuzzy Based Models for the Evaluation of Fish Habitat Quality and Instream Flow Assessment". en. In: p. 7.

Joseph, Liana N., Richard F. Maloney, and Hugh P. Possingham (2009). "Optimal Allocation of Resources among Threatened Species: A Project Prioritization Protocol". In: *Conservation Biology* 23.2, pp. 328–338. ISSN: 08888892. DOI: 10.1111/j.1523-1739.2008.01124.x.

Kendy, Eloise, Colin Apse, and Kristen Blann (Oct. 2012). *A Practical Guide to Environmental Flows for Policy and Planning*. en. Tech. rep., p. 74.

Kukkonen, S. and J. Lampinen (Sept. 2005). "GDE3: The Third Evolution Step of Generalized Differential Evolution". In: *2005 IEEE Congress on Evolutionary Computation*. Vol. 1, 443–450 Vol.1. DOI: 10.1109/CEC.2005.1554717.

Lane, Belize A., Helen E. Dahlke, Gregory B. Pasternack, and Samuel Sandoval-Solis (Apr. 2017). "Revealing the Diversity of Natural Hydrologic Regimes in California with Relevance for Environmental Flows Applications". In: *JAWRA Journal of the American Water Resources Association* 53.2, pp. 411–430. ISSN: 1093-474X. DOI: 10.1111/1752-1688.12504.

Lane, Belize, Noelle Patterson, Leo Qiu, Samuel Sandoval, Sarah Yarnell, Robert Lusardi, Julie Zimmerman, Eric Stein, Larry Brown, Theodore Grantham, and Jeanette Howard (Dec. 2019). *Functional Flows Calculator v2.31*. University of California, Davis. Davis, CA.

Lowe, Lisa, Joanna Szemis, and J. Angus Webb (2017). "Uncertainty and Environmental Water". en. In: *Water for the Environment*. Elsevier, pp. 317–344. ISBN: 978-0-12-803907-6. DOI: 10.1016/B978-0-12-803907-6.00015-2.

Luke, Sean (2013). *Essentials of Metaheuristics*. Second Edition.

Maier, H.R., Z. Kapelan, J. Kasprzyk, J. Kollat, L.S. Matott, M.C. Cunha, G.C. Dandy, M.S. Gibbs, E. Keedwell, A. Marchi, A. Ostfeld, D. Savic, D.P. Solomatine, J.A. Vrugt, A.C. Zecchin, B.S. Minsker, E.J. Barbour, G. Kuczera, F. Pasha, A. Castelletti, M. Giuliani, and P.M. Reed (Dec. 2014). "Evolutionary Algorithms and Other Metaheuristics in Water Resources: Current Status, Research Challenges and Future Directions". en. In: *Environmental Modelling & Software* 62, pp. 271–299. ISSN: 13648152. DOI: 10.1016/j.envsoft.2014.09.013.

Maloney, Kelly O., Colin B. Talbert, Jeffrey C. Cole, Heather S. Galbraith, Carrie J. Blakeslee, Leanne Hanson, and Christopher L. Holmquist-Johnson (Feb. 2015). "An Integrated Riverine Environmental Flow Decision Support System (REFDSS) to Evaluate the Ecological Effects of Alternative Flow Scenarios on River Ecosystems". en. In: *Fundamental and Applied Limnology / Archiv für Hydrobiologie* 186.1, pp. 171–192. ISSN: 1863-9135. DOI: 10.1127/fal/2015/0611.

Mathews, Ruth and Brian D. Richter (Dec. 2007). "Application of the Indicators of Hydrologic Alteration Software in Environmental Flow Setting". en. In: *JAWRA Journal of the American Water Resources Association* 43.6, pp. 1400–1413. ISSN: 1752-1688. DOI: 10.1111/j.1752-1688.2007.00099.x.

Moyle, Peter B., Joseph D. Kiernan, Patrick K. Crain, and Rebecca M. Quiñones (May 2013). "Climate Change Vulnerability of Native and Alien Freshwater Fishes of California: A Systematic Assessment Approach". en. In: *PLOS ONE* 8.5, e63883. ISSN: 1932-6203. DOI: 10.1371/journal.pone.0063883.

Muth, Robert T., Larry W. Crist, Kirk E. LaGory, John W. Hayse, Kevin R. Bestgen, Thomas P. Ryan, Joseph K. Lyons, and Richard A. Valdez (Sept. 2000). *Flow and Temperature Recommendations for Endagered Fishes in the Green River Downstream of Flaming Gorge Dam*. Tech. rep. Project FG-53. Upper Colorado River Endangered Fish Recovery Program, p. 343.

Nebro, A. J., J. J. Durillo, J. Garcia-Nieto, C. A. Coello Coello, F. Luna, and E. Alba (Mar. 2009). "SMPSO: A New PSO-Based Metaheuristic for Multi-Objective Optimization". In: *2009 IEEE Symposium on Computational Intelligence in Multi-Criteria Decision-Making(MCDM)*, pp. 66–73. DOI: 10.1109/MCDM.2009.4938830.

Null, Sarah E, Marcelo A Olivares, Felipe Cordera, and Jay R Lund (in review). "Pareto Optimality and Compromise for Environmental Water Management". en. In: *Proceedings of the National Academy of Sciences*, p. 18.

Patterson, Noelle, Belize A. Lane, Samuel Sandoval-Solis, Gregory B. Pasternack, and Qiu Yexuan (In Review). "A Hydrologic Feature Detection Algorithm to Quantify Seasonal Components of Flow Regimes". In:

Poff, N. LeRoy, J. David Allan, Mark B. Bain, James R. Karr, Karen L. Prestegaard, Brian D. Richter, Richard E. Sparks, and Julie C. Stromberg (Dec. 1997). "The Natural Flow Regime". en. In: *BioScience* 47.11, pp. 769–784. ISSN: 00063568, 15253244. DOI: 10.2307/1313099.

Poff, N. Leroy, Brian D. Richter, Angela H. Arthington, Stuart E. Bunn, Robert J. Naiman, Eloise Kendy, Mike Acreman, Colin Apse, Brian P. Bledsoe, Mary C. Freeman, James Henriksen, Robert B. Jacobson, Jonathan G. Kennen, David M. Merritt, Jay H. O'keeffe, Julian D. Olden, Kevin Rogers, Rebecca E. Tharme, and Andrew

Warner (2010). "The Ecological Limits of Hydrologic Alteration (ELOHA): A New Framework for Developing Regional Environmental Flow Standards". en. In: *Freshwater Biology* 55.1, pp. 147–170. ISSN: 1365-2427. DOI: 10.1111/j.1365-2427.2009.02204.x.

Poff, N. Leroy and Julie K. H. Zimmerman (2010). "Ecological Responses to Altered Flow Regimes: A Literature Review to Inform the Science and Management of Environmental Flows". en. In: *Freshwater Biology* 55.1, pp. 194–205. ISSN: 1365-2427. DOI: 10.1111/j.1365-2427.2009.02272.x.

Purkey, David, Marisa Escobar Arias, Vishal Mehta, Laura Forni, Nicholas Depsky, David Yates, and Walter Stevenson (July 2018). "A Philosophical Justification for a Novel Analysis-Supported, Stakeholder-Driven Participatory Process for Water Resources Planning and Decision Making". en. In: *Water* 10.8, p. 1009. ISSN: 2073-4441. DOI: 10.3390/w10081009.

Rheinheimer, David, Sarah M. Yarnell, and Joshua Viers (Oct. 2012). "Hydropower Costs Of Environmental Flows And Climate Warming In California's Upper Yuba River Watershed". In: *River Research and Applicatiions*. DOI: 10.1002/rra.2612.

Salski, A (2003). "Ecological Applications of Fuzzy Logic". In: *Ecological Informatics: Understanding Ecology by Biologically-Inspired Computation*. Berlin ; New York: Springer, pp. 3–14.

Sanderson, J. S., N. Rowan, T. Wilding, B. P. Bledsoe, W. J. Miller, and N. L. Poff (Nov. 2012). "Getting to Scale with Environmental Flow Assessment: The Watershed Flow Evaluation Tool". en. In: *River Research and Applications* 28.9, pp. 1369–1377. ISSN: 15351459. DOI: 10.1002/rra.1542.

Santos, N.R., J.V.E. Katz, P.B. Moyle, and J.H. Viers (2014). "A Programmable Information System for Management and Analysis of Aquatic Species Range Data in California". In: *Environmental Modelling and Software* 53. ISSN: 13648152. DOI: 10.1016/j.envsoft.2013.10.024.

Sun, Tao, Heyue Zhang, Zhifeng Yang, and Wei Yang (Jan. 2015). "Environmental Flow Assessments for Transformed Estuaries". en. In: *Journal of Hydrology* 520, pp. 75–84. ISSN: 0022-1694. DOI: 10.1016/j.jhydrol.2014.11.015.

Tennant, Donald Leroy (July 1976). "Instream Flow Regimens for Fish, Wildlife, Recreation and Related Environmental Resources". In: *Fisheries* 1.4, pp. 6–10. ISSN: 0363-2415. DOI: 10.1577/1548-8446(1976)001⟨0006:IFRFFW⟩2.0.CO;2.

Tharme, R. E. (Sept. 2003). "A Global Perspective on Environmental Flow Assessment: Emerging Trends in the Development and Application of Environmental Flow Methodologies for Rivers". In: *River Research and Applications* 19.5-6, pp. 397–441. ISSN: 15351459. DOI: 10.1002/rra.736.

Yarnell, Sarah M., Geoffrey E. Petts, John C. Schmidt, Alison A. Whipple, Erin E. Beller, Clifford N. Dahm, Peter Goodwin, and Joshua H. Viers (2015). "Functional Flows in Modified Riverscapes: Hydrographs, Habitats and Opportunities". In: *BioScience* 65.10, pp. 963–972. ISSN: 15253244. DOI: 10.1093/biosci/biv102.

Yarnell, Sarah M, Eric D Stein, Rob A Lusardi, Julie Zimmerman, Ryan A Peek, Theodore Grantham, Belize A Lane, Jeanette Howard, and Samuel Sandoval-solis (2018). "An Ecologically Based Approach for Selecting Flow Metrics for Environmental Flow Applications". In: *Proceedings of the 12th International Symposium on Ecohydraulics*.

Yarnell, Sarah, Ryan Peek, Gerhard Epke, and Amy Lind (2016). "Management of the Spring Snowmelt Recession in Regulated Systems". en. In: *JAWRA Journal of the*

American Water Resources Association 52.3, pp. 723–736. ISSN: 1752-1688. DOI: 10.1111/1752-1688.12424.

Yarnell, Sarah, Eric Stein, Angus Webb, Ted Grantham, Julie Zimmerman, Ryan Peek, Belize Lane, Jeanette Howard, and Samuel Sandoval-Solis (2020). "A Functional Flows Approach to Selecting Ecologically Relevant Flow Metrics for Environmental Flow Applications". In: *River Research and Applications*.

Yarnell, Sarah, Julie Zimmerman, Robert Lusardi, Alyssa Obester, Ryan Peek, Nick Santos, Theodore Grantham, Jeanette Howard, Eric Stein, and Kristine Taniguchi-Kwan (Oct. 2019). *The California Environmental Flows Framework: A Guidance Document for Users. Draft Version 1.*

Young, W. J, D. C. L Lam, V Ressel, and I. W Wong (Mar. 2000). "Development of an Environmental Flows Decision Support System". en. In: *Environmental Modelling & Software* 15.3, pp. 257–265. ISSN: 1364-8152. DOI: 10.1016/S1364-8152(00)00012-8.

Zamani Sabzi, Hamed, Shabnam Rezapour, Rachel Fovargue, Hernan Moreno, and Thomas M. Neeson (Feb. 2019). "Strategic Allocation of Water Conservation Incentives to Balance Environmental Flows and Societal Outcomes". en. In: *Ecological Engineering* 127, pp. 160–169. ISSN: 09258574. DOI: 10.1016/j.ecoleng.2018.11.005.

Zimmerman, Julie K. H., Daren M. Carlisle, Jason T. May, Kirk R. Klausmeyer, Theodore E. Grantham, Larry R. Brown, and Jeanette K. Howard (Jan. 2018). *California Unimpaired Flows Database v0.1.1.* San Francisco CA: The Nature Conservancy.

Zitzler, Eckart, Marco Laumanns, and Lothar Thiele (May 2001). *SPEA2: Improving the Strength Pareto Evolutionary Algorithm.* en. Tech. rep. Computer Engineering and Networks Laboratory (TIK), p. 21.